Polybutadiene Copolymers via Atomistic and Systematic Coarse-Grained Simulations

Anastassia Rissanou,[1,2,*] Antonis Chazirakis,[1,2]

Patrycja Polinska,[3] Craig Burkhart,[4]

Manolis Doxastakis,[5] Vagelis Harmandaris[1,2,6,*]

1. Institute of Applied and Computational Mathematics (IACM), Foundation for Research and Technology Hellas, (FORTH), IACM/FORTH, GR-71110 Heraklion, Greece.
2. Department of Mathematics and Applied Mathematics, University of Crete, GR-71409, Heraklion, Crete, Greece.
3. Goodyear S.A., Avenue Gordon Smith, Colmar-Berg L-7750, Luxembourg.
4. The Goodyear Tire and Rubber Company, 142 Goodyear Blvd., Akron, Ohio 44305, USA.
5. Department of Chemical and Biomolecular Engineering, University of Tennessee, Knoxville, Tennessee 37996, USA.
6. Computation-based Science and Technology Research Center; The Cyprus Institute, Nicosia 2121, Cyprus.

Abstract

The systematic coarse graining of polymeric systems is a usual route in order to extend the range of spatiotemporal scales and systems accessible to molecular simulations. Here we present a bottom-up methodology in order to obtain coarse-grained (CG) models for copolymers, derived from more than one species of monomers via detailed atomistic simulations. In the proposed scheme each monomer type is represented as a different CG particle. The effective CG interactions are obtained via a dual stage multi-component iterative Boltzmann inversion (IBI) optimization scheme, in which the single component terms of the CG model are obtained from homopolymer simulations, whereas the interactions between different CG type particles (mixed terms of the CG model) from the simulation of a symmetric composition copolymer. As an example, the proposed optimization scheme is applied on polybutadiene (PB) copolymers consist of cis-1,4, trans-1,4 and vinyl-1,2 isomers. The derived CG PB copolymer model is examined with respect to its transferability across molecular weight and the copolymer composition. In addition, using the newly derived CG model various PB copolymers across a broad range of cis-1,4, trans-1,4 and vinyl-1,2 compositions are examined. Structural and dynamical properties of PB copolymers are presented. The vinyl component is found to have a large impact on the conformational properties of PB copolymer melts because of the different packing imposed by side groups. Standard composition mixing rules are used to predict the time mapping factors used for the calculation of both segmental and center-of-mass dynamics of the PB copolymer, coming from the CG model.

1. Introduction

Polymer-based materials constitute a class of complex systems characterized by a very broad range of spatiotemporal scales, which need to be probed in order to predict their macroscopic properties directly from the monomeric structure. To address this challenge, complementary to experimental methods, simulation methodologies, across various scales, are valuable tools. In this aspect, atomistic simulations can provide direct, quantitative predictions of structure-property relations of such complex systems. However, the range of polymeric systems that can be studied in full atomistic detail is still limited due to the extreme computational cost associated with their study. To extend the range of accessible scales, as well as systems, various mesoscopic (coarse-grained, CG) polymer models have been proposed that reduce the systems' degrees of freedom, based on either top-down or bottom-up parameterization schemes.[1-13] In top-down CG approaches, the parameters for the effective CG interactions are derived using typically experimental data about macroscopic properties.[14-16] On the contrary, bottom-up CG models are developed using information from the more detailed level of description—i.e., from atomistic, or even quantum, simulations.[13, 17-28]

The advantage of systematic, bottom-up CG models is that, in principle, they retain the chemical information at the mesoscopic length scales and allow a quantitative investigation of specific polymeric systems. In such models a molecule, or a part of the polymer chain (e.g. a monomer), is mapped to a coarser representation, where it is described as a CG particle or "super atom." Thus, the dimensionality of the system is reduced, allowing for the study of the model systems over longer length and time scales, compared to the all-atom ones. In these approaches, typically CG effective potentials are calculated by approximating the (many body) potential of mean force (PMF)[29,30] using data from detailed atomistic simulations. Different methods can be used for the numerical parameterization of the CG effective interaction. For example, force matching (FM) is based on a mean least squares problem that considers as observable function the total force acting on each CG particle.[26, 31-33] The relative entropy (RE) is another parametrization method, which employs the minimization of the relative entropy.[34-36] A family of very popular methods to derive the CG effective interaction for polymeric systems is based on parametrizing structural distribution functions; examples include

direct inverse Boltzmann (DBI)[6, 17], the inverse Monte Carlo (IMC)[37-38] and the iterative Boltzmann inversion (IBI).[8] In IBI effective potentials are obtained through an iterative procedure in order to reproduce the (intra- and inter-molecular) structure (distribution functions) of the CG polymer chains, as they are calculated from long atomistic simulations.[8-9, 11, 39] In the last one to two decades, CG models of various polymers have been developed based on such structural-based methods.[9, 17-18, 22, 24, 40-44]

A very important class of polymeric materials is that of copolymers derived from more than one species of monomers. Copolymers are directly related to important technological applications; for example they are utilized as thermoplastic elastomers, pressure sensitive hot-melt adhesives, drug delivery systems, in the field of nano-patterning and surface modification,[45-46] polymer mixing[47], etc. Various studies based on analytical[48-52] or computational methods[53-54] have explored the properties of random copolymers, their phase behavior and the order-disorder transition demonstrating the significance of their structural and chemical correlations.[48-49, 55] In all these studies, due to the underlying chemical complexity, the need for accurate models is highlighted. Among copolymers, polybutadiene (PB) one holds an exceptional positon in rubber industry. The monomeric structure of PB includes the cis-1,4, trans-1,4 and vinyl-1,2 isomers. PB systems of various microstructures have been widely studied experimentally through dielectric spectroscopy,[56] NMR[57] and neutron scattering methods.[58-59]

Furthermore, PB systems have been the subject of many computational studies where their structural, conformational and dynamical properties have been extensively explored.[60-65,66] Usually PB homopolymers are examined. A bottom up approach for coarse graining was applied on cis- and trans- PB,[67] using the dissipative particle dynamics strategy of Hijón et al.[68], achieving an accurate description of structural properties.

Moreover, numerous simulation studies investigated nanocomposites with PB using organic nanofillers, like graphene[69-71] or inorganic nanofillers, like silica. [72-76] The last case finds extensive application in elastomers. The largest and the most important portion of tires is that of the polymeric material. PB constitutes one of the typical rubber compounds (butadiene rubber, BR)[77] whereas poly-cis-1,4 isoprene[78] and styrene-butadiene rubbers (SBR)[79-80] are also widely used. The BR and SBR cases refer to

copolymer chains which are composed of various types of polymers. The properties of these systems are strongly dependent on their composition.[81]

In a recent publication Baba et al.[82] proposed a method for parametrizing bead spring models, using atomistic data, by modifying the bending potential of the standard Kremer-Grest model, and by introducing empirical functions to describe the dependence of the structural parameters of the polymer chains on the molecular weight. The methodology was applied on random PB copolymers and on SBR polymers. Comparisons between fully atomistic and CG MD simulation results were presented for both structural and dynamical properties and corresponding conversion parameters are extracted. The modified bead-spring models were found to accurately describe the structure of copolymers above a characteristic length, of the order of Kuhn segment.

However up to now, a systematic CG procedure for PB copolymers, taking into account all the degrees of freedom (i.e., bonded and non-bonded interactions) for various PB microstructures, is still missing. At the same time, a detailed investigation of the properties of PB copolymers as a function of their chemical composition via atomistic simulations is a challenging task due to the high computational demands. The present work aims along the above two directions: i) To develop a systematic bottom-up CG model for PB copolymers of various microstructures, using data directly from atomistic simulations. This is a highly non-trivial issue considering that the CG effective potentials are, as mentioned above, approximations of the free energy (many-body PMF) and thus it is expected to depend on the actual composition of a copolymer. To address this challenge, we implement a multi-component (simultaneous) optimization IBI approach using intra- and inter- molecular distribution functions. With this approach a library of CG effective interaction (potentials) is developed for PB copolymers of any composition, comprised of all three isomers. In addition, the molecular weight and composition transferability of the derived CG PB copolymer potentials is examined. ii) To investigate the phase space of composition of PB copolymers in terms of cis-, trans- and vinyl proportions is the second objective. A series of CG molecular dynamics runs explore the effect of composition on various structural and dynamical properties of the PB copolymer melts.

The rest of the paper is organized as follows: The simulation models are described in Section 2. More specifically information about the atomistic model is given in subsection 2.1 and details for the simulation runs are given in subsection 2.2. Section 3 contains a detailed step-by-step description of the systematic bottom-up approach for the development of the CG copolymer model. Properties of random PB copolymers of various microstructures, obtained from CG simulations are presented in Section 4. Discussion and concluding remarks are contained in Section 5.

2. Model Systems and Simulations

2.1. Development of Force Field (ff)

Atomistic model: PB chains of various microstructures are described through a united atom (UA) model[76] shown in Table SI-1 up to Table SI-6. It is highly based on a UA model proposed by Smith and Paul,[61, 83] which has been developed mainly for cis-1,4 and trans-1,4 PB. A slight modification for the potential describing the dihedral angle around double bonds (CH2-CH=CH-CH2) has been performed, in order to avoid a low percentage of, unphysical at the given conditions, cis/trans isomerization. In more detail, as it has been described in our previous publication[76], the original dihedral potential has been substituted by a harmonic improper dihedral potential which preserves the correct stereochemistry.

Furthermore, since the original UA PB model has been developed for cis-1,4 and trans-1,4 isomers, it provides an inadequate description of the vinyl-1,2 one. More specifically, MD simulations of pure atactic vinyl-1,2 PB melts, using the original model, predict a density of about 20% larger, compared to the one derived from an all-atom PB model using the COMPASS II,[84] a detailed, many-body force field. To correct for such discrepancies, the non-bonded energetic interactions of the UA PB model, for the vinyl-1,2 isomer, were modified. After a series of simulation runs with different values of ε-parameter of the Lennard-Jones (LJ) potential, the values, which better reproduce the density of vinyl-1,2 PB melts, derived from the all-atom runs, have been chosen. These values were found to be around 40% smaller than the original ones. The new values of the LJ potential for the UA vinyl-1,2 PB model are shown in Table SI-2 of the

Supporting Information. In the following we will use the abbreviations cPB, tPB and vPB for cis-1,4, trans-1,4 and vinyl-1,2 PB correspondingly.

2.2. Simulation Details

Initial atomistic configurations of PB homopolymers and copolymers are generated via an in-house script which constructs a number of random copolymer chains containing all three isomers of butadiene. Chains are in a united-atom representation, therefore the term atomistic refers to united atoms. 30mer and 100mer polymer chains have been utilized in the current study. Since a main part of the current work concerns the development of a systematic methodology for deriving CG models of copolymers, the chain lengths were chosen in order to ensure full relaxation in the atomistic scale. Note that the 100mer correspond to 400 UA groups per chain and to mildly entangled (co)polymer PB melts. A detailed investigation of higher molecular weights, via the CG model, will be the topic of a future work. All chains are different in terms of composition in such a way that the average melt composition being equal to the desired one. After generation, each system is thoroughly equilibrated by performing energy minimization followed by MD runs of about ~50-100ns. Then production runs are performed in the NPT statistical ensemble, at T=433K, well above the bulk T_g of model PB chains.[85] Nose-Hoover thermostat[86-87] and Parrinello-Rahman barostat[88] were used for controlling temperature and pressure (p = 1atm), respectively. Atomistic production runs of about 200ns were performed, with a time step for the integration of the equations of motion equal to 1fs. For the CG runs, a time step from 2fs up to 5fs was used, and the simulation times were up to about 300 ns. Frequency of sampling is set such that ~ 4000 – 5000 configurations are collected for the analysis. The time of 50-100ns and 200-300ns used respectively for the equilibration and production runs are well above the maximum relaxation times of the cPB, tPB and vPB systems, which are of the order of ~10ns for all three systems (see Figure SI-13). Cut-off distances of 1nm and 1.5nm for atomistic and CG runs, respectively, are used for the truncation of the non-bonded interactions, which are coming as a result of the model parameterization in each case. Van der Waals tail corrections were applied for energy and pressure.[89] CG particles are in general larger than the UA groups, thus exhibit stronger cohesive, van der Waals-based dispersion interactions. Thus, typically the cutoff length

used in CG models is larger than in the UA ones. Qualitatively we expect that, in order to not loose large part of the dispersion interactions, the cutoff length should correspond to a length where there is no any structural correlation in the CG level. All MD simulations have been performed by the open source GROMACS software.[90-91]

3. Systematic Coarse-Grained Model for PB Copolymers

In the following, a general procedure for the development of a CG model for copolymers derived from more than one species of monomers is given. The proposed multi-component optimization scheme is applied to PB copolymers with various microstructures, where one monomer is mapped to one CG particle.

First, a specific functional (basis set) representation of the CG effective potential is proposed. Following, standard (decoupling) assumptions of the CG degrees of freedom, typically used in polymer literature, the many-body PMF is approximated as a sum of bonded and non-bonded interactions. The bonded interactions concern neighboring CG particles along the same polymer chains: (a) "bonding" that refer to 2 consecutive particles (1-2 interactions), (b) "angular" 3 consecutive particles are participating (1-3 interactions) and (c) "dihedral" in which 4 consecutive particles are involved (1-4 interactions). The non-bonded CG (pair) interactions are between CG particles belonging in different chains, or within the same polymer chain but more than 3 CG bonds apart from each other. Here we use the standard pair approximation for the non-bonded interaction potential between CG particles. Many body effects are partially described by the iterative procedure. An explicit incorporation of the latter, via three-body terms,[92-94] or density dependent potentials[38] would be possible, however increases the computational cost of the derived CG models. This would be a topic of a future investigation."

Based on the above, if we assume N_c polymer chains, with $N_{ac}(k)$ number of CG particles (monomers) per chain k, and n_{bonds}, n_{angles}, $n_{dihedrals}$ being the total number of bonds, angles and dihedrals in the CG representation, respectively, the entire effective interaction potential in the CG copolymer system can be written as:

$$U^{CG}(\boldsymbol{q}) = U^{CG}_{bonded}(\boldsymbol{q}) + U^{CG}_{non-bonded}(\boldsymbol{q}) \qquad (1)$$

$$U^{CG}_{bonded}(\boldsymbol{q}) = U^{CG}_{bonds}(\boldsymbol{r}) + U^{CG}_{angles}(\boldsymbol{\theta}) + U^{CG}_{dihedrals}(\boldsymbol{\varphi}) \qquad (2a)$$

$$U_{bonds}^{CG}(\boldsymbol{r}) = \sum_{i=1}^{n_{bonds}} V_b^{n(i),m(i)}(r_i), \tag{2b}$$

$$U_{angles}^{CG}(\boldsymbol{\theta}) = \sum_{i=1}^{n_{angles}} V_a^{n(i),m(i),k(i)}(\theta_i) \tag{2c}$$

$$U_{dihedrals}^{CG}(\boldsymbol{\varphi}) = \sum_{i=1}^{n_{dihedrals}} V_d^{n(i),m(i),k(i),l(i)}(\varphi_i) \tag{2d}$$

$$U_{non-bonded}^{CG}(\boldsymbol{q}) = \sum_{k=1}^{Nc} \sum_{i=1}^{Nac(k)-1} \sum_{j=i+4}^{Nac(k)} V_{nb}^{n(i),m(j)}(|\boldsymbol{q}_i - \boldsymbol{q}_j|) +$$
$$\sum_{k=1}^{Nc-1} \sum_{l=k+1}^{Nc} \sum_{i=1}^{Nac(k)} \sum_{j=1}^{Nac(l)} V_{nb}^{n(i),m(j)}(|\boldsymbol{q}_i - \boldsymbol{q}_j|) \tag{3}$$

where $\boldsymbol{q}$ represents the coordinates of the (NC) CG particles ($\boldsymbol{q} = \{\boldsymbol{q}_1, \ldots, \boldsymbol{q}_{NC}\}$) and $\boldsymbol{r}, \boldsymbol{\theta}$ and $\boldsymbol{\varphi}$ is the set of CG bonds, angles and dihedrals. $n(i)$, $m(i)$, $k(i)$, $l(i)$ are, for a given interaction i, the type of the CG particles (here different isomers) participating in it: $\{n, m, k, l\} = \{T, C, V\}$. The CG non-bonded interaction consists of intra- and inter-molecular contributions described via the two terms in the right hand part of Eq. (3).

It is clear from the above equations (1)-(3) that to obtain the total effective CG interaction, i.e., the CG force field, all the different terms inside the sums, which describe the interaction of specific types of CG bonds, angles and dihedrals, are required. This is a highly non-trivial optimization problem for a case of a copolymer with different types of CG particles, due to the large number of terms needs to be considered. For example, for the specific case of PB copolymer, consisting of 3 different isomers, considered here, there are 6 types of bonding, 18 types of angular and 45 types of dihedral interactions, as well as 6 types of non-bonded interactions need to be obtained. Moreover, it is well known that the decoupling approximation, discussed above, is only partially valid and particularly, at small length scales, the above bonded and non-bonded interactions are expected to be correlated.[17] Therefore, in principle, all the CG interaction terms, shown in Eqs. (2), (3), should be simultaneously optimized.

To address the above challenge, which as mentioned is inherit to all systematic CG approaches of multi-species polymeric systems, we follow a two-stage procedure, using results from atomistic simulations of various PB homopolymers and a single PB copolymer, of an almost symmetric composition as shown in Figure 1: (a) In the first stage the terms in Eqs (2) and (3) that correspond to the same type of CG particles (here isomers), are obtained using structure information (distribution functions) from the

homopolymer runs. (b) In the second stage, the interactions between different types of CG particles are derived, using data from the atomistic simulation of a single PB copolymer. To achieve this we first construct a UA PB copolymer of 30mer polymer chains of symmetric composition, 34:33:33 in Trans:Cis:Vinyl (T:C:V) number of monomer percentage. In this part, the various bonded and non-bonded cross-term interactions (i.e., cis-trans, cis-vinyl, and trans-vinyl), are optimized while the same component (cis-cis, trans-trans, vinyl-vinyl) ones are taken from the corresponding homopolymer systems, obtained in stage (a). In all cases a non-parametric form of the CG effective interactions is assumed using tabulated potentials.
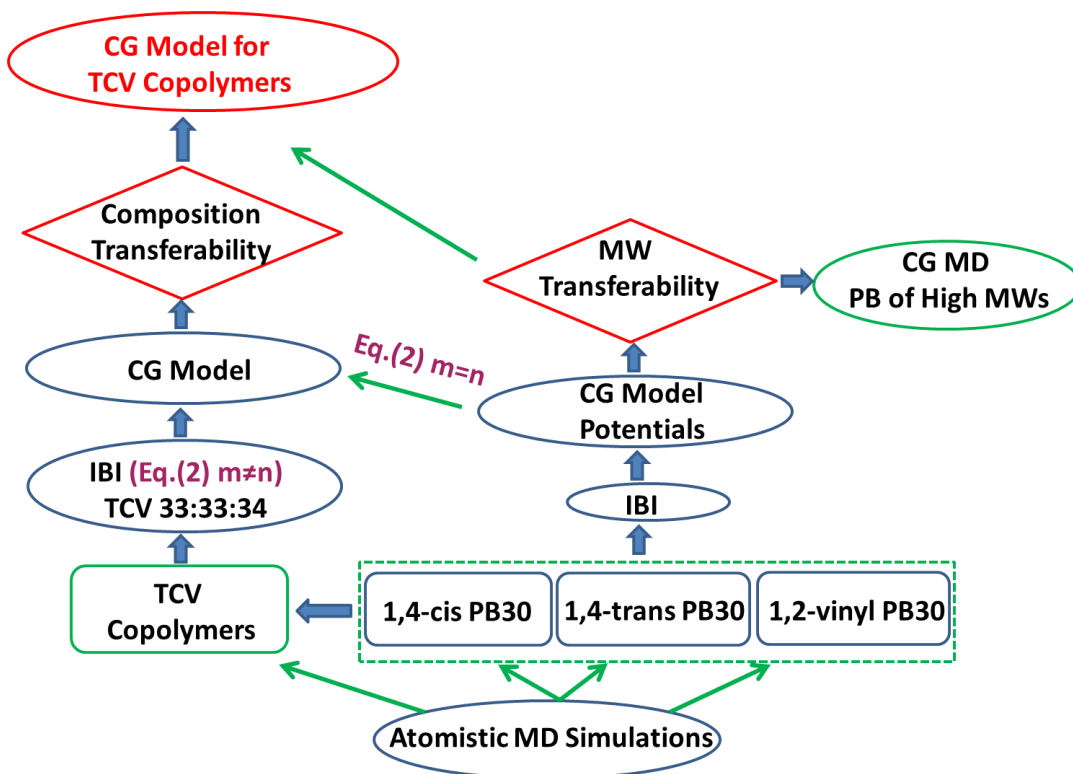
Figure 1: Flow chart for the systematic bottom-up development of a CG model for copolymers of more than one species of monomers. Here the methodology is applied to PB copolymers of various (cis-1,4, trans-1,4 and vinyl-1,2) microstructures.

The last part of the multi-component optimization procedure concerns the validation of the CG copolymer model and the examination of its transferability across systems with different molecular weights and compositions, i.e., outside of the systems

used for their derivation (training dataset). For each case, the predictions of the CG PB model concerning structural properties of PB homopolymers and copolymers are directly compared against the predictions of the underlying UA PB model. First, higher molecular lengths of 100mer are used to examine transferability of the CG model to higher molecular weights. Second, two additional PB copolymers with different composition of the three components (i.e., T:C:V 25:25:50 and 10:10:80) are simulated with both UA and the CG models, to examine the ability of the CG model to reproduce the properties of PB copolymers with different composition than the one used for the derivation of the CG model. A flow chart of the overall procedure is schematically represented in Figure 1. Below the two stages of the optimization procedure are described in detail.

3.1. PB Homopolymers

In the first part of the proposed optimization procedure, the homopolymer (same component) terms of the CG effective interaction potential are obtained, using data from independent atomistic simulations of all cPB, tPB, and vPB homopolymers.

Atomistic simulations: Pure component systems of all PBs stereochemistries are described in Table 1 and the corresponding monomeric structures are presented in Figures 2a-c for cPB, tPB and vPB monomers accordingly. For vPB three isomers (i.e., isotactic (Iso); syndiotactic (Syndio); atactic) have been simulated. Results concern polymer chains of 30 monomers at 433K. Density values predicted by the current model are also found in good agreement with data obtained from all-atom PB simulations using the COMPASS II force field[84] (data not shown here). In addition, the experimental density value (0.90 g/cm^3) for cPB at 298K[95-96] is in excellent agreement with the predictions of the current model (0.91 g/cm^3).[76] The density of the PB homopolymers are close to each other, with the cPB exhibiting a slightly larger value than vPB, and mainly than tPB. Moreover, tPB has slightly larger chain dimensions (radius of gyration, R_G) than the cPB, whereas the vPB has the smallest R_G, as expected due to the side group.

The radius of gyration of three vinyl isomers indicate more extended conformation of syndiotactic isomer compared to isotactic and atactic ones. Moreover, considerably higher is the characteristic ratio of syndiotactic vPB denoting a stiffer molecule. Isotactic chains are of smaller dimensions and of higher flexibility whereas

atactic lies in between the two isomers. For cPB and tPB similar characteristic ratios are found.

Table 1. Density (ρ) and structural properties for all PB stereochemistries for 30mer polymer chains.

System	T(K)	ρ(g/cm^3)	R_G(nm)	C_{30}
cPB	433	0.835±0.04	1.44±0.03	5.09±0.41
tPB	433	0.795±0.03	1.51±0.04	5.51±0.46
vPB (Iso)	433	0.819±0.04	0.99±0.01	4.55±0.28
vPB (Syndio)	433	0.815±0.04	1.23±0.002	7.80±0.51
vPB (Atactic)	433	0.816±0.03	1.05±0.02	5.09±0.34

CG model of PB homopolymers: The mapping of the atomistic to the CG representation corresponds each monomer to one CG particle, as presented schematically in Figure 2d for vPB. The atom codes of the corresponding united atoms (CV1, CV2, CDV1, CDV2), used in the description of force field (Table SI-1 – Table SI-6), are also given; similar, as well, is the notation for the other monomer types. There are 3 different types of CG particles that correspond to the different isomers: cPB, tPB and vPB.
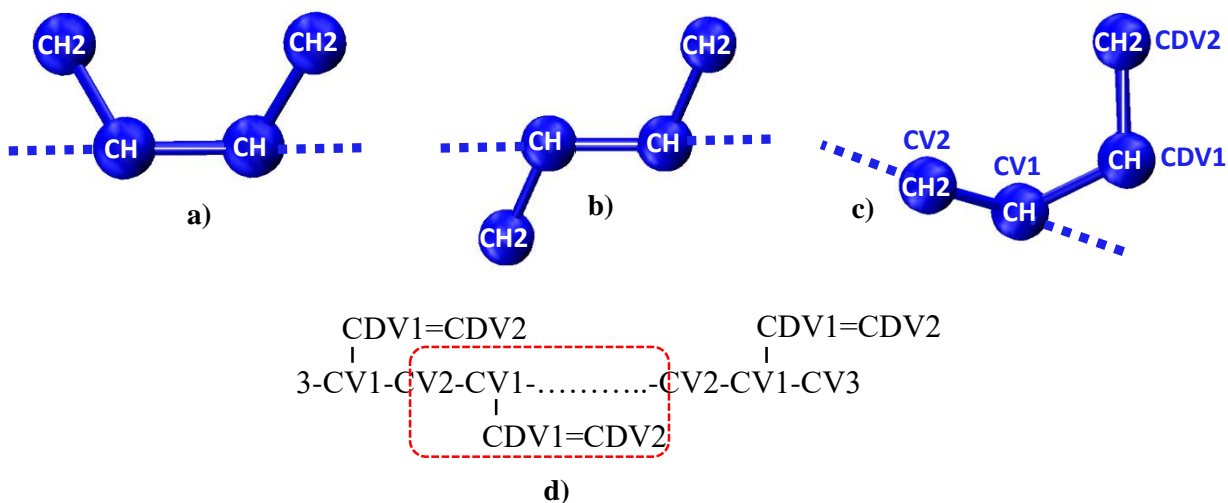
Figure 2: Snapshots of PB monomers of a) cPB, b) tPB, and c) vPB accordingly. d) Mapping of vPB from the atomistic to the CG representation (one monomer corresponds to one CG particle). United atoms are referred with their code names accordingly; show in Figure 2c and in SI as well.

The effective interaction between the CG particles is developed following a multi-component optimization scheme based on IBI method.[3, 8, 39] In this method, the CG potentials are obtained from the distribution functions of the various structural CG degrees of freedom, which are extracted from the atomistic simulations; the latter are denoted as target distributions. In the current CG PB copolymer model, we consider: (a) two-body (CG bonds), (b) three-body (CG angles), (c) four-body (CG dihedrals) and (d) pair CG non-bonded contributions. After the derivation of the target distributions, the initial corresponding CG potentials are calculated assuming Boltzmann statistics. Then, CG runs are performed and the new CG distributions are computed. Convergence of all distributions to the corresponding target ones is achieved through a numerical iterative process, applying correction on the potentials at each step. The number of iterations cannot be specified in advance. The convergence of distributions is examined via the minimization of corresponding merit functions. The whole procedure is as follows: (a) First, for a few iterations, the various components of each CG interaction type are independently updated, starting from the bonding, angular, dihedral up to the non-bonded ones. (b) Second, due to the coupling of the different terms, many iterations were all components are simultaneously updated are performed, to ensure accurate prediction of all structural distribution functions. (c) Finally, a few iterations of updating all distributions together with a pressure coupling term are necessary, to reproduce the correct pressure (see Eq. SI-10). Detailed description of the optimization method is provided in the Supporting Information.

As an example of this procedure, in Figures 3a-d the distributions of the CG degrees of freedom for atactic 30mer vPB are displayed, after the convergence of the above described optimization algorithm. Distributions of CG bonds are shown in Figure3a, of CG angles in Figure3b, of CG dihedrals in Figure 3c and of non-bonded pair radial distribution function (rdf), g(r), in Figure 3d. In all cases, the distributions are in excellent

agreement with the corresponding curves of the atomistic runs (target distributions), obtained by mapping the atomistic configurations in the CG representation, demonstrating the proper convergence of the optimization procedure. Similar agreement is found for all distributions which correspond to the cPB and tPB homopolymers.
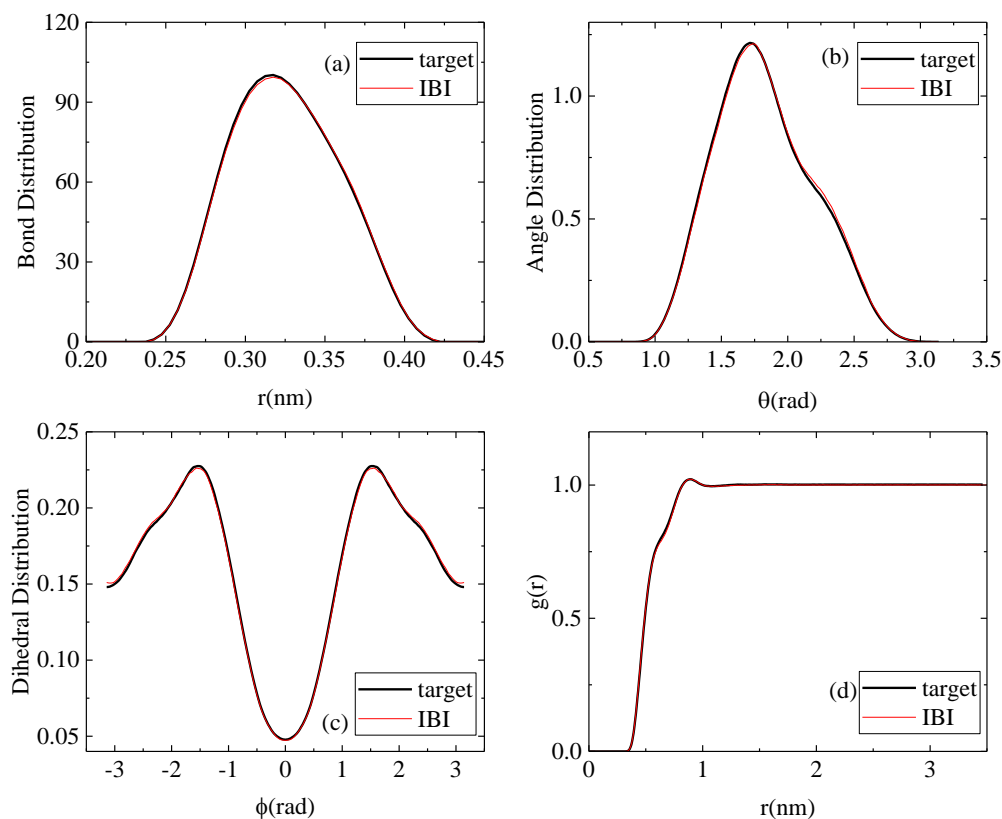
Figure 3: The distributions of the various degrees of freedom for atactic 30mer vPB at 433K; (a) bonds, (b) angles, (c) dihedrals and (d) nonbonded pair radial distribution function.

The overall optimization procedure is evaluated through the total merit function, which has been minimized for all components simultaneously including the pressure correction. The total merit functions as a function of iterations for the three isomers of vPB are presented in Figure SI-1. Values of the order ~0.03 are attained with the pressure fluctuating around 1atm.

Molecular weight transferability of the CG PB model: One major challenge for all CG models is their ability to be accurate for systems outside the ones used for their parametrization, i.e., the training dataset. For polymeric systems in particular, it is very important for the CG models to describe systems of longer polymer chains (higher molecular weight, *M*). To examine this, we perform CG dynamic simulations of systems with higher *M* using the CG effective interactions developed above, based on short (30mer) chains.

In the following results for melts of 100mer polymer chains for cPB, tPB and (atactic) vPB are presented. As mentioned above, for such systems long UA simulations have been also performed to directly examine the transferability of the CG model at high *M*. Atomistic and CG simulation results are compared against various measures. First, the non-bonded pair radial distribution, g(r), between the center-of-mass (cm) of the monomers is presented in Figures 4a-c for cPB, tPB and vPB atactic melts respectively, as it is calculated from the atomistic runs. Each curve is compared to the corresponding g(r) between CG beads (i.e., particle in the CG representation ⇔ four united atoms), obtained from the CG runs. An excellent superposition of curves is observed verifying that the CG model describes accurately the polymer structure for all three stereochemistries and the produced CG potential is transferable, with respect to the local structure, across *M*. Similar is the agreement for the bonded distributions as well (data not shown here).

Moreover, to further examine the predictions of the CG PB model, with respect to the thermodynamic properties and chain dimensions we present in Table 2, the density, the radius of gyration, the end-to-end distance and the characteristic ratio for the 100mer polymer chains of cPB, tPB and vPB atactic, from both atomistic and CG simulations. Again a very good agreement among the predictions of the two models for all systems is observed. Note also here that the experimental value for the characteristic ratio (4.61 g/cm^3) for cPB at 298K[95] is in good agreement with the predictions of the current model for 100mer polymer chains calculated as (C_{100} = 4.85±0.4).

A comparison among the three isomers reveals a higher peak in the rdf of cPB compared to tPB, although at almost the same position, which indicates a better packing

for cis chains. Note, also, that in vPB the peak moves at longer distances pointing to a looser packing which is attributed to its side group.
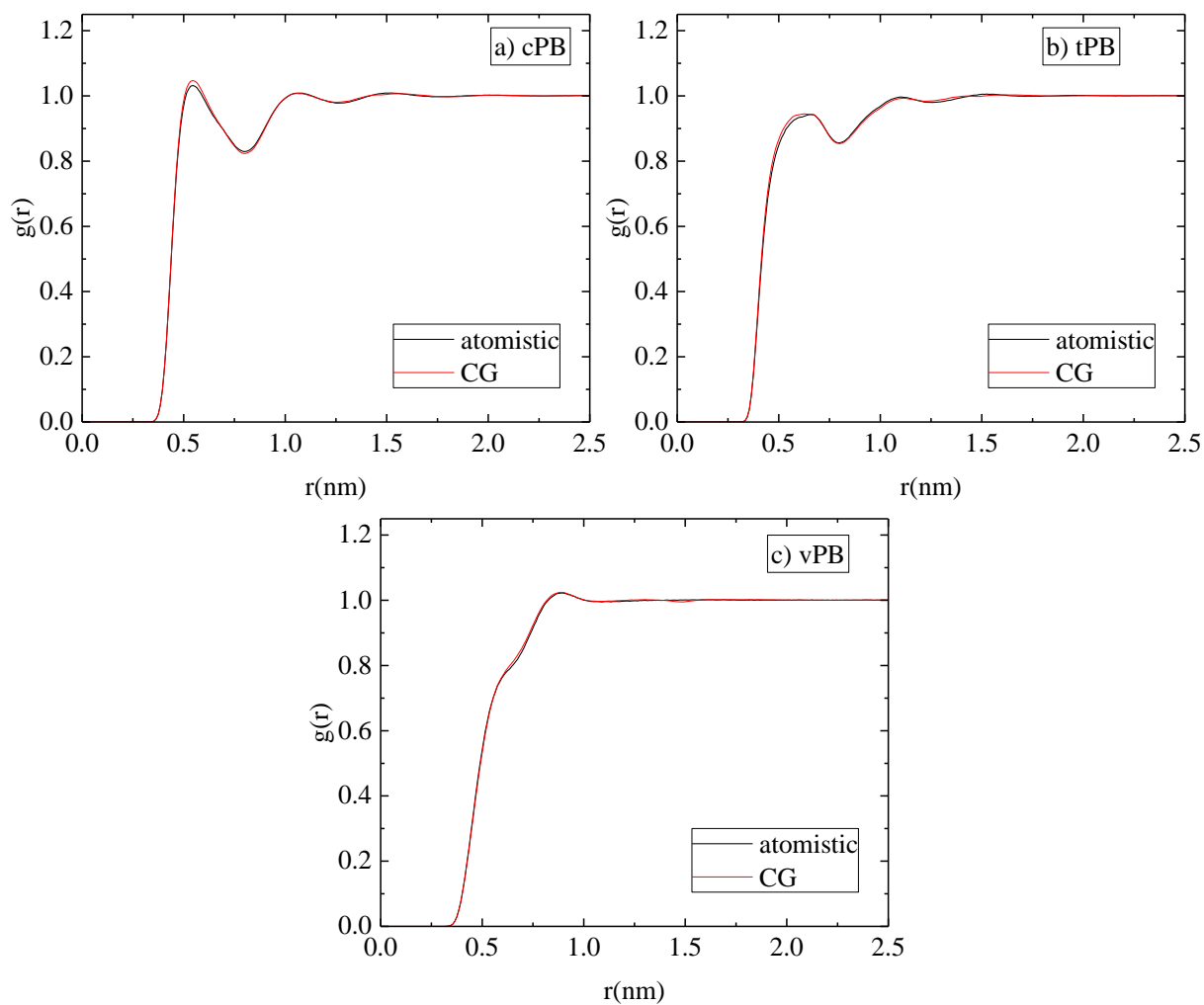
Figure 4: Total pair radial distribution function (rdf) of 100mer PBs between the cm of monomers in atomistic representation and between the CG beads in CG simulations for (a) cPB, (b) tPB and (c) vPB atactic at 433K.

Table 2. Density and structural properties of cPB, tPB and vPB atactic at 433K, 100mer polymer chains in both atomistic and CG representation.

System	$\rho(g/cm^3)$	$R_G(nm)$	R_{ee} (nm)	C_{100}
Atomistic				
cPB	0.843±0.02	2.70±0.05	6.57±0.23	5.02±0.35
tPB	0.812±0.03	2.91±0.05	7.17±0.22	5.96±0.37
vPB (Atactic)	0.846±0.03	1.99±0.03	4.96±0.15	5.53±0.19
CG				
cPB	0.846±0.03	2.85±0.06	7.07±0.23	5.85±0.37
tPB	0.810±0.04	2.86±0.07	7.02±0.28	5.76±0.46
vPB (Atactic)	0.853±0.04	2.06±0.05	5.10±0.20	5.78±0.44

3.2. PB Copolymers

The second stage of the multi-component optimization procedure is used to derive CG models for copolymers. This concerns the CG interaction potential between different types of CG particles (monomers), i.e., the mixed terms in Eqs. (2) and (3). For that, data from atomistic simulations of PB copolymers are used. In general, PB (random) copolymers comprised of all three stereochemistries of PBs (Trans:Cis:Vinyl, T:C:V) in various proportions; here, T:C:V values are percentages in number of different repeat units. The extension of the CG models of pure components to copolymers is a very intriguing subject, since as mentioned in the introduction the CG potential is a parametrization of the free energy of the system. The main challenge is to represent the free energy based on individual contributions from CG interactions, parametrized on single-component systems, to copolymers of different compositions. To address this challenge, a series of different compositions of Trans:Cis:Vinyl (T:C:V) components, almost symmetrically chosen, are examined, as presented in Figure 5.
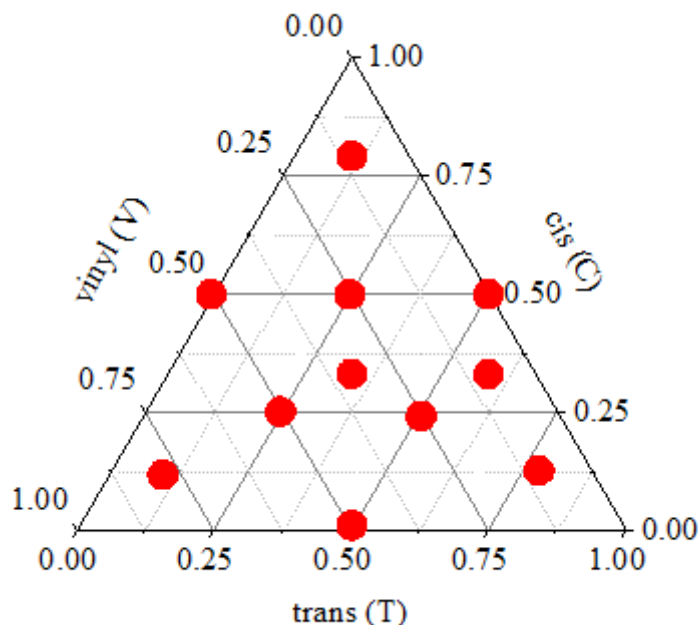
Figure 5: Schematic representation for the different compositions of copolymer PBs studied here.

Atomistic simulations of PB copolymers: We start with atomistic simulations on some selected compositions for 30mer polymer chains at 433K, which are presented in Table 3. The corresponding densities, the radii of gyration and the end-to-end distances are also included. Differences in the dimensions of polymer chains indicate conformational changes induced by the composition. First, it is clear that the more the vinyl component, the smaller the chain dimensions. This is to be expected due to the side group of vPB, and is also observed in the homopolymers among different isomers (see Table 2). Second, an increase of the vinyl component leads to a small increase of density. The composition dependence of the non-bonded pair radial distribution between the cm of monomers, g(r), is presented in Figure 6. A gradual decrease of the first peak with the increase of vinyl component is observed whereas the first minimum becomes shallower. A different arrangement of chains is attained when vinyl proportion rises, which becomes more pronounced beyond 50% of vinyl. Side groups of vinyl monomers impose larger spaces as it is clearly shown in the 10:10:80 system, where the peak is moved at much longer distances. Few experimental data exist which can be almost directly compared with our

simulation results. Corresponding comparisons of quite similar systems/conditions are provided in Table SI-7.

Table 3. Density and structural properties for 30mer T:C:V copolymers of different compositions from atomistic and CG MD simulations, at 433K.

Copolymer T:C:V ratio	$\rho(g/cm^3)$	$R_G(nm)$	R_{ee} (nm)	C_{30}
Atomistic				
50:50:0	0.82	1.52±0.16	3.80±0.16	5.64±0.46
60:30:10	0.83	1.47±0.03	3.69±0.14	5.57±0.42
34:33:33	0.85	1.34±0.03	3.35±0.13	5.15±0.40
25:25:50	0.85	1.28±0.03	3.20±0.12	5.19±0.39
10:10:80	0.84	1.13±0.02	2.81±0.10	4.95±0.35
CG				
34:33:33	0.84	1.35±0.03	3.37±0.03	5.37±0.41
25:25:50	0.83	1.29±0.03	3.22±0.04	5.44±0.41
10:10:80	0.82	1.16±0.02	2.89±0.03	5.45±0.39
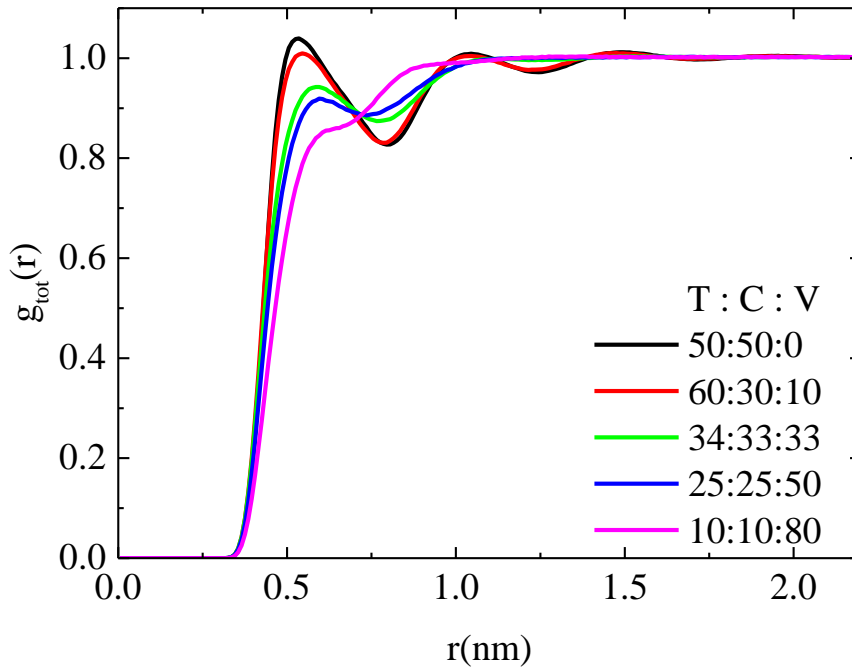
Figure 6: Pair radial distribution functions between the cm of monomers of PB copolymers with various microstructures (T:C:V compositions) at 433K.

CG potential for PB copolymers: Next, we develop the CG effective interaction "mixing terms," i.e., between CG particles (monomers) of different microstructure. To achieve this, an almost symmetric system (i.e., ~equal proportion of the three components, {T:C:V}={33:33:34}) is used for the construction of a CG potential through the IBI procedure. Note that for vinyl component an atactic isomer is used. The various bonded and non-bonded cross-term distributions are produced (i.e., cis-trans, cis-vinyl, trans-vinyl), while the distributions for cis-cis, trans-trans and vinyl-vinyl terms are taken from the corresponding pure systems. Comparisons between target and CG distributions for the non-bonded pair radial distributions, after the end of the iterative optimization procedure, are presented in Figures 7a-f.
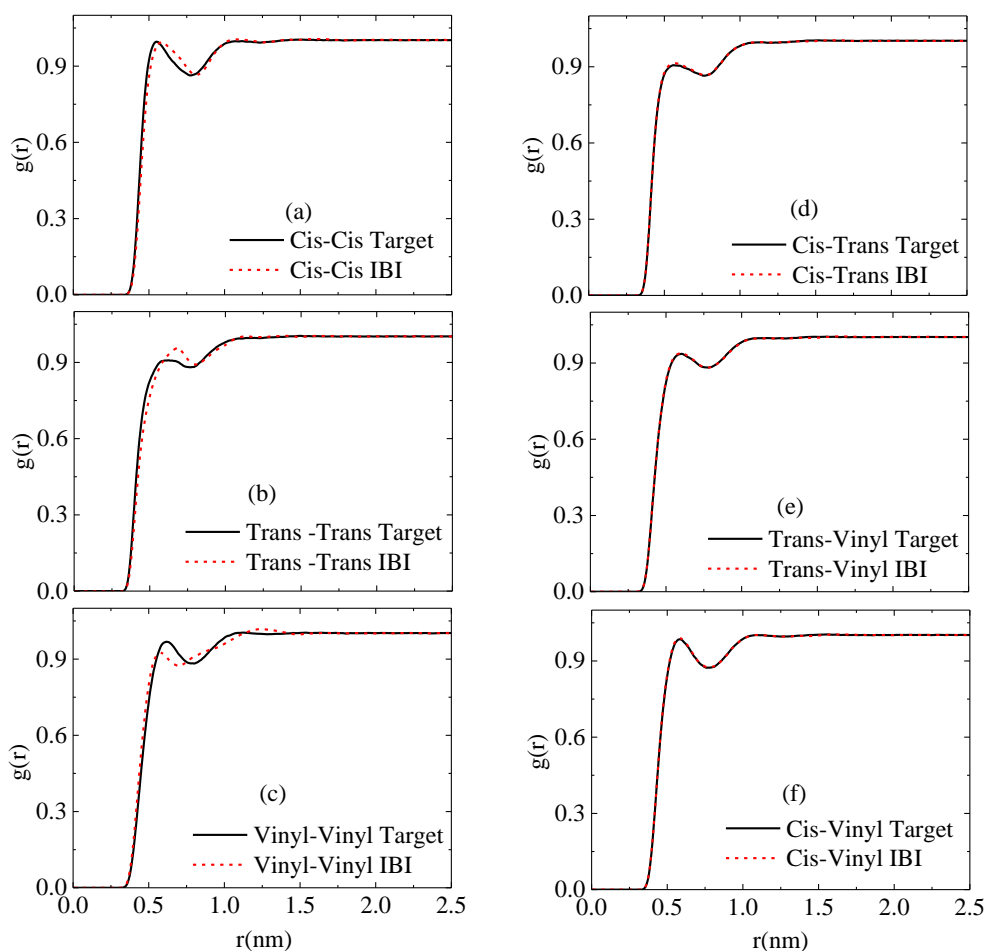
Figure 7: Radial distribution function (rdf) of 30mer PB copolymers with T:C:V composition 33:33:34 at 433K. Comparison of target curves (atomistic) and IBI results; (a-c) same pair components (d-f) cross-term components.

In more detail, in Figures 7d-e the cross terms are presented where the distributions are identical with the target ones, as expected since the potential is optimized over these distributions. Small discrepancies are observed in the distributions of same component pairs (Figures 7a-c), where the optimization has not been applied. However, such differences have a very minor effect in the total CG potential, so we choose to proceed with the current potentials. Analogous comparisons for some representative combinations of the bonded degrees of freedom are presented in Figures SI-2 for bonds, Figure SI-3 for angles and Figure SI-4 for dihedrals. A similar picture,

where small deviations exist in the distributions of same component pairs, is also observed, providing satisfactory results for the respective potentials.

An overall evaluation of the optimization procedure followed to derive the CG potentials is displayed in Figure 8, where the minimization of the total merit function with time is presented. Minimization for all distributions is performed simultaneously together with pressure correction, which finally fluctuates around 1atm.
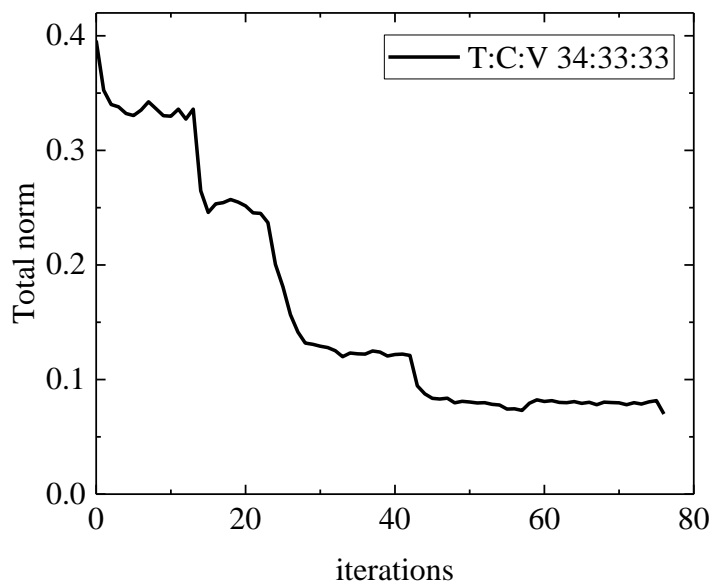
Figure 8: Total merit function for bonds, angles, dihedrals and non-bonded interactions together with pressure correction for PB copolymer 30mer T:C:V 34:33:33 at 433K.

Transferability of CG PB copolymer model across composition range: In the following, the CG potentials for PB copolymer, derived from the multi-component IBI optimization scheme using atomistic data from the (three) homopolymers and a single PB copolymer T:C:V 34:33:33, are used for the simulation of two other systems of copolymers with different compositions: (a) 30mer PB T:C:V 25:25:50, and (b) 30mer PB T:C:V 10:10:80. The various properties of CG runs are compared with the corresponding ones coming from atomistic simulation runs of the same systems. Figures 9a-c present the total non-bonded pair radial distribution, $g(r)$, as well as its intra-molecular, $g_{intra}(r)$, and inter-molecular, $g_{inter}(r)$, components, for the PB T:C:V 25:25:50 system, calculated both from

the CG and the UA PB copolymer simulations. A very good agreement between UA and CG data is observed for all distributions.

A more detailed picture for the various components of rdf is shown in Figures 10a-f: Correlations between same type of monomers are shown in Figures 10a-c, whereas the cross-correlations are shown in Figures 10d-f. Again the agreement is very good for all curves. Agreement between atomistic and CG distributions is quantified through Eq. SI-9 and the average total merit function of the six pairs is 0.01.
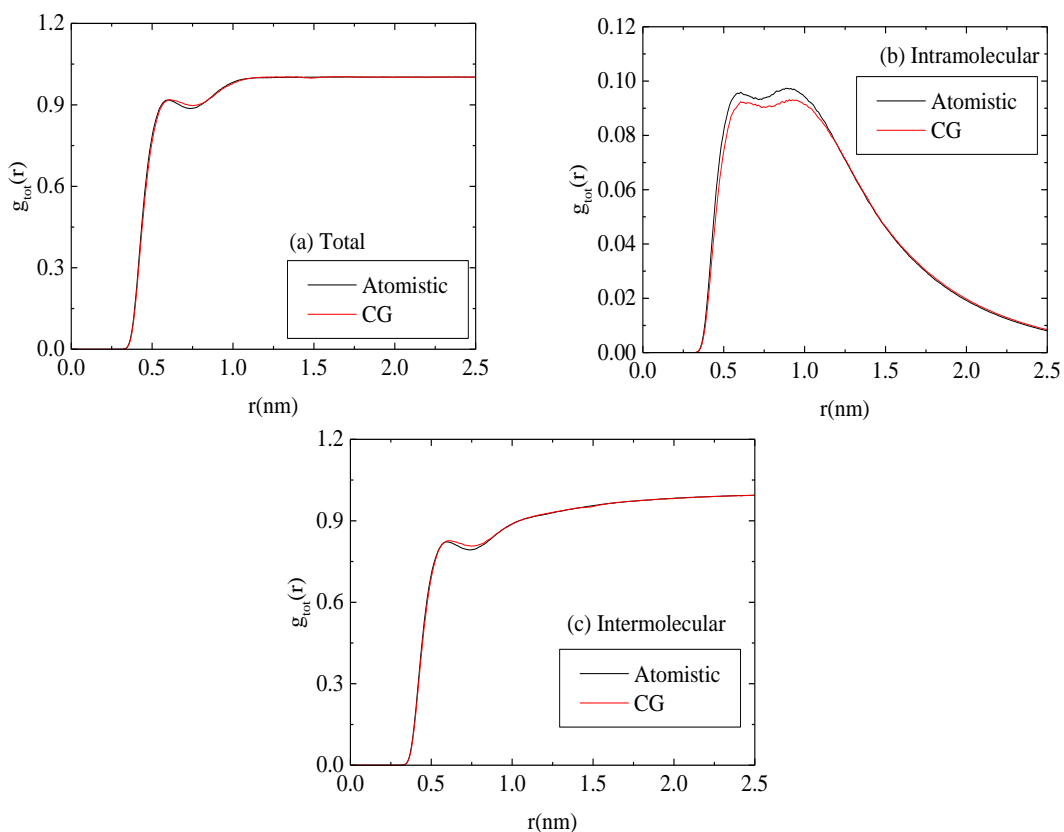
Figure 9: Radial distribution function (rdf) of 30mer PB copolymers of T:C:V composition 25:25:50 at 433K. Comparison of atomistic and CG results; (a-c) total rdf, intramolecular and intermolecular parts respectively.
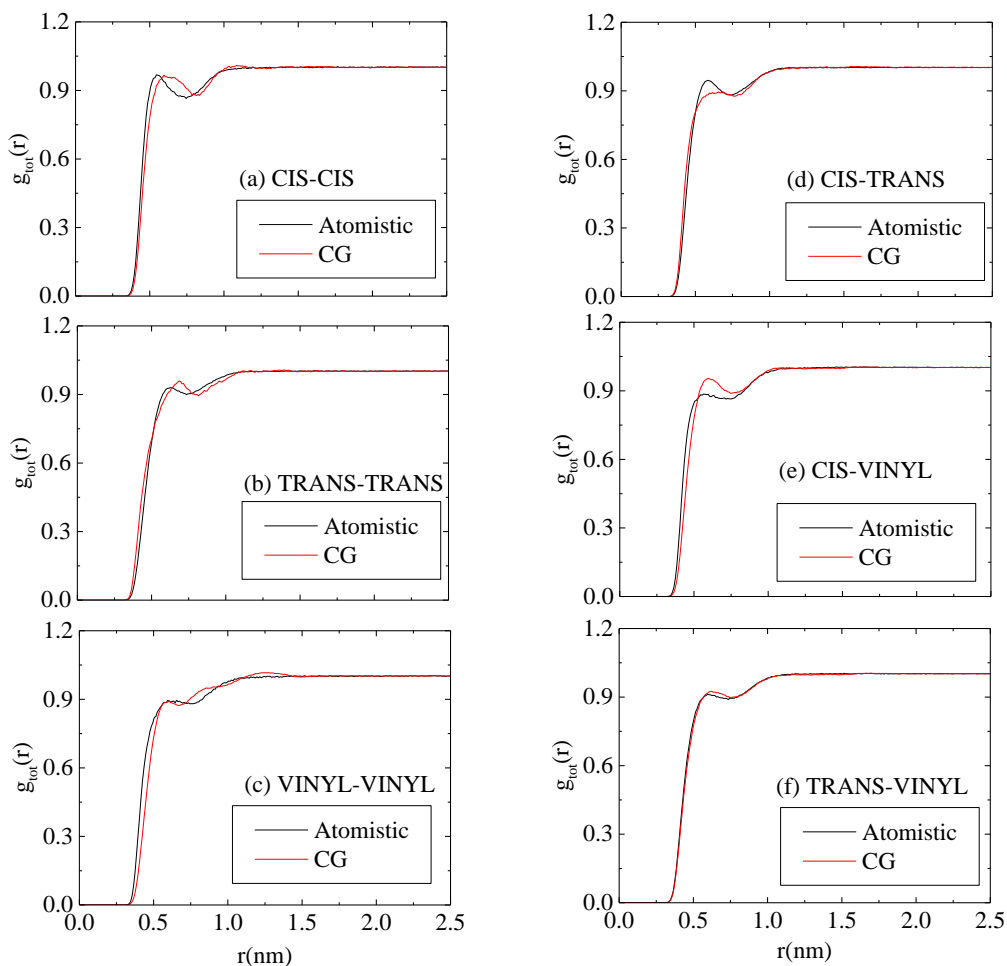
Figure 10: Radial distribution function (rdf) of 30mer PB copolymers of T:C:V composition 25:25:50 at 433K. Comparison of atomistic and CG results; (a-c) same pair components, (d-f) cross term components.

Similar is the agreement for the bonded degrees of freedom; data for the 25:25:50 (T:C:V) PB copolymer, are presented in Figures SI-5, Figure SI-6 and Figure SI-7 for bonds, for angles and for dihedrals accordingly. Same behavior is observed in the 10:10:80 PB copolymer (data not shown here). Structural properties of both 25:25:50 (T:C:V) PB and 10:10:80 PB copolymers systems at 433K are summarized in Table 3. Comparison of atomistic simulation data with the corresponding ones coming from the CG representation for R_{ee}, R_G and the characteristic ratio for 30mer (C_{30}) show good agreement within statistical uncertainties. Overall, the above data confirm that the CG model, derived from the multi-stage optimization IBI approach, provides a very good

description of the local structure in PB (random) copolymers of different isomer composition. The value of the total merit function at the end of the optimization procedure for the systems where IBI was applied (i.e., 30mer cPB, tPB, vPB homopolymer systems and the 34:33:33 and 60:30:10 copolymer systems at 433K) are given in Table SI-8 of the Supporting Information. A small increase of total merit function is observed in copolymers compared to homopolymer systems. However, in all cases, total merit functions attain values lower than $\sim 10^{-1}$.

## 4. Properties of PB random copolymers

4.1. Structural and Conformational Properties

In the following, the properties of (unentangled) PB random copolymers are further investigated, for various compositions, using the derived CG PB model. CG simulations of a full set of different composition copolymers (see Figure 5) are performed and various properties are calculated. Polymer chains comprised of 30 units are simulated in the NPT statistical ensemble at pressure of 1atm and temperature of 433K. Further simulation details are given above (see section 2.2). The copolymer compositions were chosen to scan the entire ternary composition diagram. In addition, a few systems suggested as a typical proportion in experiments (e.g. T:C:V 60:30:10)[97], have been also studied.

First, the structure of the PB copolymer melts is investigated through non-bonded pair radial distributions, g(r), between CG beads (monomers), shown in Figures 11b-c. For all systems, the bonded (intramolecular 1-2, 1-3 and 1-4) contributions are excluded. As reference systems we also present the g(r) data for the three (cPB, tPB, vPB) homopolymers in Figure 11a, which have also been discussed in the previous section (see Figure 4).

In the following, the dependence of the local structure (packing) of the PB copolymer chains, quantified via g(r) correlations, on the composition range is examined. For this, we study the different copolymers as a function of the increase of the percentage for each isomer along the chain. First, we examine how the local packing in PB copolymer is changing by increasing the amount of vPB component. In Figure 11b g(r) data for copolymers with vinyl proportion ranges from 0% up to 100% (vPB atactic

homopolymer) are presented and three well defined regimes are signified; 0%, [10-33]% and [80-100]% with a gradual transition among them. The first and last regimes are the vinyl-free (PB copolymers without vinyl-1,2 component) and vinyl-rich systems respectively, whereas the middle regime includes cases of poor up to intermediate vinyl concentrations. Up to 33% of vinyl, decrease in the height of the first peak compared to the vinyl-free copolymer is observed, with a simultaneous decrease of the depth of the first minimum. In addition, the position of the first peak is slightly moved to longer distances. The 50% vinyl curve moves towards the same direction whereas in the 80% vinyl a clear differentiation is observed, with almost loss of the first peak which appears, much weaker, at much longer distances (i.e., from ~0.54nm to ~0.87nm), approaching the vinyl homopolymer system.
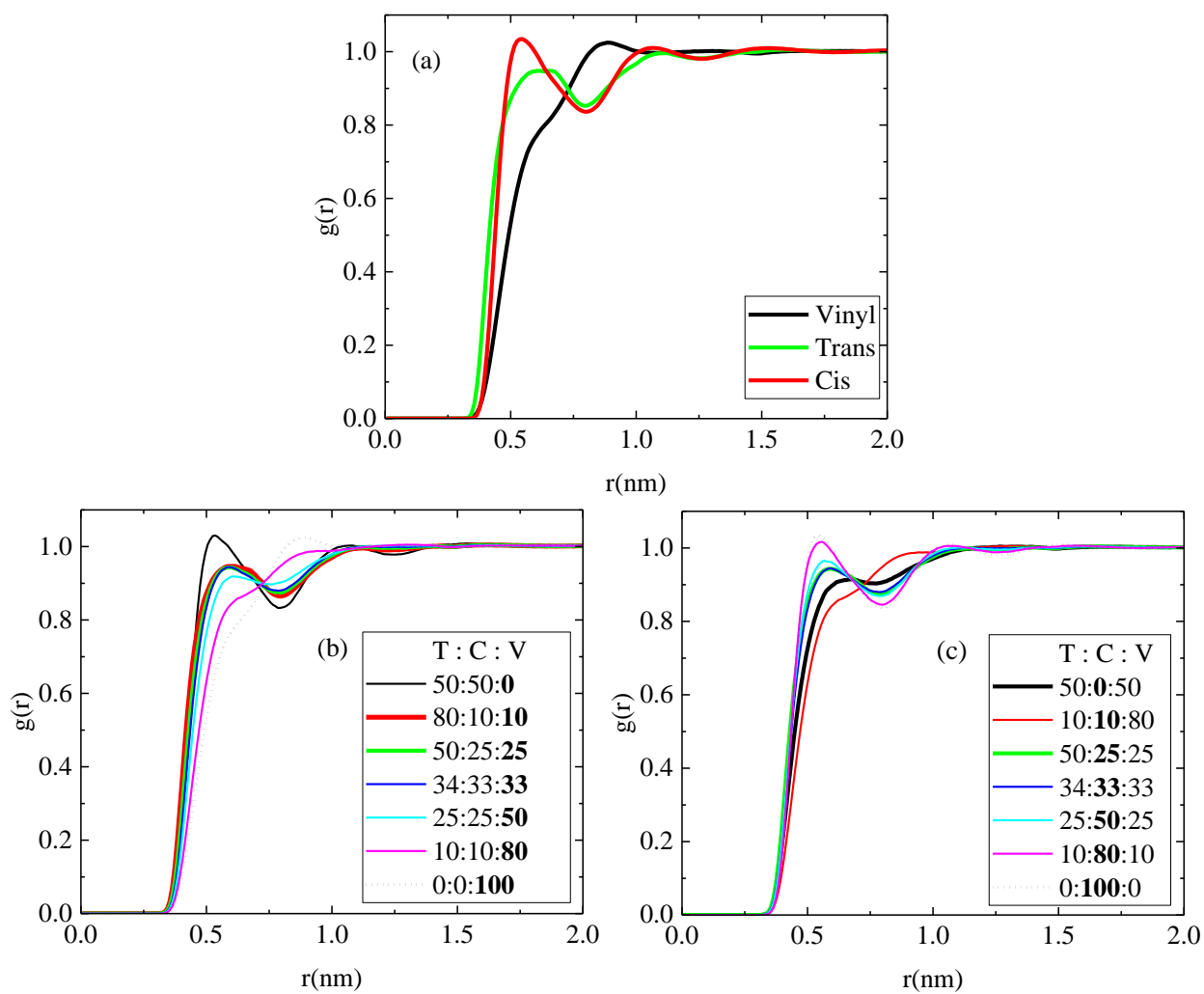
Figure 11: Radial distribution function (rdf) of 30mer PB polymers with various T:C:V proportions at 433K. (a) homopolymers (b) increasing percentage of vinyl stereochemistry (c) increasing percentage of cis stereochemistry.

Moreover, the model PB copolymers can be examined as a function of the increase of cis or trans proportion. In Figure 11c the g(r) of all copolymers are presented as a function of the increase of cis component. Starting from the cis homopolymer, which has the highest first peak among the three homopolymer systems, a gradual decrease of cis composition leads to a corresponding decrease of the height of the first peak and of the depth of the first minimum of g(r) curves. At the same time, the curve which corresponds to the vinyl-rich system (i.e., 10:10:80) differentiates from all the rest approaching to the one of the vinyl homopolymer. In Figure SI-8 the copolymers analyzed as a function of the increase of the trans component. Milder differences among the curves are observed, except for the one which corresponds to the 10:10:80 system. Moreover, for enhanced cis population (i.e., 25:50:25), the first peak is higher in agreement with the homopolymers correlations (Figure 11a). Based on the above, interestingly enough, it seems that the vinyl component strongly affects the local packing of PB copolymer melts because of its side group, which imposes a much different arrangement of chains at higher distances.

An additional measure which quantifies intramolecular packing in polymer melts is the packing length, p,[98-99] which is defined as the ratio of the occupied volume of a chain over its mean square end-to-end distance ($p = \dfrac{M}{\langle R_{ee}^2 \rangle \rho N_A}$), where M is the molar mass and N_A the Avogadro's number. This parameter expresses the intrinsic elasticity of a polymer and attains values of a few Angstroms for common polymers.[98] Values for packing lengths are presented in Table 4. The regimes detected in g(r) for the series of systems with increasing vinyl amount are also reflected in packing lengths, which are larger in vinyl-rich chains. This increasing trend has also been found experimentally, though experimental data are referred to lower temperatures and higher molecular weights.[99-100] Among pure systems, for cPB and tPB packing lengths are very similar, whereas for vPB it is higher as a result of its side group.

The density (ρ) and the chain dimensions (R_G) of the CG PB copolymers are also given in Table 4. Again the systems are analyzed as a function of the increase of each component (vinyl-, cis- and trans-). Among homopolymers, cPB has the highest density vPB follows and tPB has the lowest density. The chain dimensions follow the opposite

order with trans attaining the larger R_G-value, cis an intermediate and vinyl the smallest one.

Moreover, in the first part of Table 4, increase of vinyl proportion leads to a gradual decrease of chain dimensions in terms of R_G values from vinyl-free up to vinyl homopolymer chains. It has to be mentioned here that results for both rdfs and structural measures are consistent with those derived from atomistic simulations of the same systems (Figure 6 and Table 3). This is also in agreement with the simulations predictions for R_G of Baba et al.[82] for low, mid and high vinyl PB copolymer chains. For cis and trans components (second and third part of Table 4 accordingly), moving from the 100% homopolymer system towards lower percentages, decrease in chain dimensions is observed up to 33% of the corresponding component, remaining larger than the component-free system. In the highest vinyl content system, R_G is considerably smaller closer to the dimensions of vinyl homopolymer.

Table 4. Density and structural properties for 30mer T:C:V copolymers of increasing percentage of vinyl/cis/trans stereochemistry at 433K from CG MD simulations.

System T:C:V	ρ(g/cm³)	p(nm)	R_G(nm)	C_{30}	Linear Mixing Rule	
					R_G(nm)	C_{30}
Increasing vPB						
50:50:**0**	0.821	0.24	1.49±0.03	5.47±0.39	1.47±0.04	5.25±0.40
80:10:**10**	0.814	0.28	1.46±0.03	5.46±0.42	1.44±0.04	5.32±0.41
50:25:**25**	0.829	0.28	1.39±0.03	5.38±0.39	1.37±0.03	5.33±0.40
34:33:**33**	0.837	0.28	1.35±0.03	5.37±0.41	1.33±0.03	5.34±0.39
25:25:**50**	0.831	0.31	1.29±0.03	5.44±0.41	1.26±0.03	5.38±0.38
10:10:**80**	0.824	0.39	1.16±0.02	5.45±0.39	1.14±0.02	5.47±0.38
0:0:**100**	0.823	0.47	1.06±0.02	5.52±0.37		
Increasing cPB						
50:**0**:50	0.794	0.28	1.32±0.03	5.69±0.42	1.28±0.03	5.42±0.39
10:**10**:80	0.824	0.39	1.16±0.02	5.45±0.39	1.14±0.02	5.47±0.38

50:**25**:25	0.829	0.28	1.39±0.03	5.38±0.39	1.37±0.03	5.33±0.40
34:**33**:33	0.837	0.28	1.35±0.03	5.37±0.41	1.33±0.03	5.34±0.39
25:**50**:25	0.848	0.29	1.37±0.03	5.26±0.40	1.36±0.03	5.30±0.39
10:**80**:10	0.849	0.28	1.42±0.03	5.28±0.40	1.42±0.03	5.24±0.38
0:**100**:0	0.831	0.24	1.45±0.03	5.19±0.38		
Increasing tPB						
0:50:50	0.854	0.28	1.28±0.03	5.35± 0.40	1.26±0.03	5.36±0.37
10:10:80	0.824	0.39	1.16±0.02	5.45±0.39	1.14±0.02	5.47±0.38
25:50:25	0.848	0.29	1.37±0.03	5.26±0.40	1.36±0.03	5.30±0.39
34:33:33	0.837	0.28	1.35±0.03	5.37±0.41	1.33±0.03	5.34±0.39
50:25:25	0.829	0.28	1.39±0.03	5.38±0.39	1.37±0.03	5.33±0.40
80:10:10	0.814	0.28	1.46±0.03	5.46±0.42	1.44±0.04	5.32±0.41
100:0:0	0.812	0.25	1.49±0.04	5.31±0.42		

The properties of random copolymers are often studied via semi-empirical rules using the properties of the homopolymers and composition (linear) mixing rules. Here, we check this assumption by presenting the predictions of such rules on the properties of the random PB copolymers. Taking into account the proportion of each isomer, the corresponding predictions for the radius of gyration and characteristic ratio of chains are presented in Table 4. The agreement between MD results and linear mixing rules predictions is rather good within the statistical accuracy (error bars are calculated based on the homopolymer data). On the contrary, linear mixing models rather underestimate the density of the PB copolymers.

Another interesting observation is among systems with the same percentage of vinyl but different cis and trans combinations (i.e., 10:80:10, 60:30:10, 80:10:10). Slightly smaller chain dimensions and higher density attains the 10:80:10 system compared to both others, where chains are of comparable size (i.e., R_G = 1.42; 1.45; 1.46 nm respectively). The analogous comparison in rdfs is presented in Figure SI-9. The first peak in rdf curve, which corresponds to 10:80:10 system, is lower and the first minimum is shallower compared to the two other systems due to the prevalence of trans population.

Furthermore, comparison among triplets of symmetric systems (i.e., 10:80:10, 10:10:80, 80:10:10 and 50:25:25, 25:50:25, 25:25:50, 50:50:0, 0:50:50, 50:0:50) indicate again the dominant effect of vinyl. In all three combinations the system with the highest content in vinyl differs from the two others bearing the smaller dimensions. Similarly the corresponding rdf curve is less structured (i.e., lower first peak) (Figure SI-10 a,b,c).

The characteristic ratio (C_{30}) is a measure of chain stiffness, which is also affected by the composition of the copolymer. Comparison of pure systems shows that vPB is stiffer than both cis and trans isomers which is again attributed to its side group. On the other hand, cPB is found as the most flexible whereas trans is in between. In copolymer chains C_{30} varies according to the composition mixing of the three isomers in a way that is also predicted by the predictions of the linear mixing model.
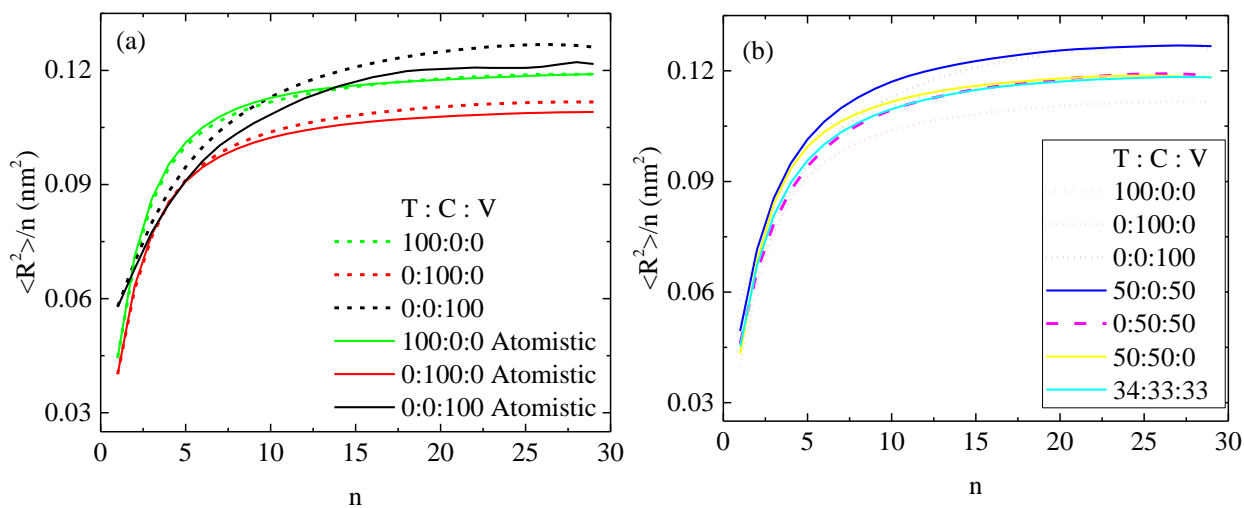
Figure 12: Internal distances as a function of monomer number for 30mer PB homopolymers and copolymers at 433K.

Furthermore, an analogous to the above behavior is observed by probing the internal distances, which are presented, as a function of the monomer distance, n, along a polymer chain, for the different PB systems in Figure 12. The internal distances are calculated as: $\langle R^2(n) \rangle = \langle [R(i) - R(i+n)]^2 \rangle$, where the statistical average is performed over all i monomers along a chain, all chains and all polymer configurations. First data about the internal distances of homopolymers from both atomistic and CG PB models are

presented in Figure 12a. Curves are in good agreement, within the statistical accuracy; results from both atomistic and CG model indicate vinyl as the stiffer component, trans follows and cis the most flexible component. In Figure 12b, the predictions about the homopolymers are compared against the results for different copolymers with two components (i.e., 50:0:50, 50:50:0 and 0:50:50) and the symmetric copolymer 34:33:33. The curve for 50:0:50 is close to the pure vinyl curve which indicates that the equal mixing trans-vinyl copolymer is of similar stiffness to the vinyl homopolymer. On the other hand, equal mixing cis-vinyl and cis-trans copolymer is as stiff as trans homopolymer. The symmetric 34:33:33 copolymer lies in between the stiff vinyl and the flexible cis homopolymer.

Overall a complete set of data for densities, dimensions and characteristic ratios, together with the conformational information through rdfs, provide an exploration of the phase space of PB copolymer composition, in terms of proportions of different stereochemistries.

4.2. Dynamics

In the following, the dynamical properties of PB random copolymers are examined via atomistic and CG simulations, for the different compositions. In order to quantitatively predict the polymer dynamics via CG models their ability to reproduce the dynamics of the underlying chemical systems should be examined. The current CG PB copolymer models are developed based solely on structural data and the friction at the CG level, associated with the missing atomistic degrees of freedom, is not taken explicitly into account in the CG equations of motion. Therefore, it is expected that the dynamics of the CG PB systems is faster than the UA PB ones.[17, 101-102] In order to "correct" for the missing friction, in a post-processing stage, a typical procedure is based on re-scaling of the CG time scale, via a time mapping factor τ_{CG} using detailed dynamic data from the atomistic simulations. For a homogeneous polymeric system, where a single monomeric friction coefficient characterizes the dynamics of all polymer chains, the time mapping factor is equivalent to the ratio of the atomistic friction coefficient, ζ_{AT} over the CG one, ζ_{CG}, i.e. $\tau_{CG} = \frac{\zeta_{AT}}{\zeta_{CG}}$. To calculate τ_{CG}, in principle, any dynamical property can be used. Here, we choose the segmental, and center-of-mass (cm), mean

squared displacement (MSD) data, which can be obtained directly from the atomistic and CG simulations. In more detail, we scale the CG segmental dynamic data in order to match the atomistic ones, at the long time regime, using a scaling factor τ_{CG}.[17, 43, 103] The time scaling factor, as a ratio of two friction coefficients, has been found to depend slightly on the chain-length and strongly on the temperature.[18, 43, 102] It is also expected to depend strongly on the monomeric structure and the (local-segmental) free energy landscape. Thus, it might be different for the different stereoisomers. Here, since we study systems at the same temperature, we compute the time mapping factor for the different PB homopolymers of the same chain length, and we examine its dependence on the PB copolymer composition.

We first examined the dynamics of the PB homopolymers predicted by the atomistic and the CG simulations. In Figures 13a-c we present the MSD of the cm of monomers (segmental dynamics) and the cm of polymer chains, as a function of time, for cPB, tPB and vPB melts respectively, coming from both atomistic and CG runs. As expected, segmental and cm dynamics coincide at the long-time regime. The segmental MSD data of the CG model are scaled by time scaling factors equal to 3.2±0.2, 6.0±0.2 and 4.16 ±0.15, for cis, trans and vinyl respectively, in order to match the corresponding atomistic ones in the long-time regime. In the current CG model we observe a larger scaling factor for tPB system, compared to cPB and vPB ones. Our hypothesis, is that due to the smaller density of tPB the (spherical) CG particles exhibit higher mobility (smaller ζ_{CG}), resulting into a larger dynamic scaling factor. As we see the CG MSDs, after scaling, re-produce accurately the dynamics of the underlying atomistic systems, over a broad range of spatiotemporal scales, apart from very short length and times. In general atomistic and CG data, for segmental MSDs, match each other for length scales above around 0.5nm and corresponding time scales of about ~20ps. Corresponding values for the cm MSDs are a few (2-4) nm for length scales and ~15ns for time scales. Note that the length scale of ~0.5nm corresponds to about the size of each CG particle.
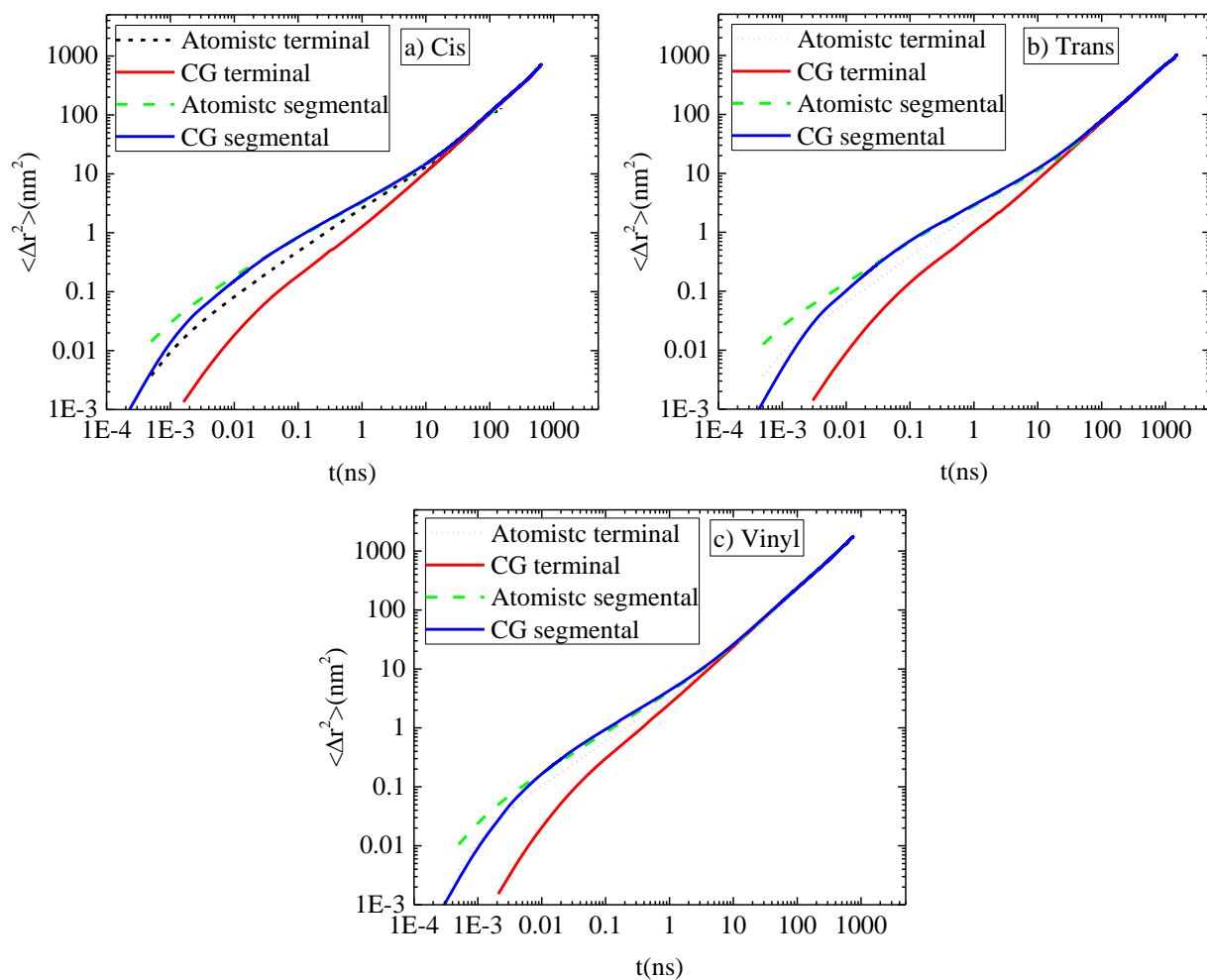
Figure 13: Mean squared displacement of monomers and of center-of-mass of PB chains as a function of time, for 30mer PB homopolymers, obtained from atomistic and CG model scaled with the corresponding τ_{CG}: (a) cPB, (b) tPB, (c) atactic vPB (T =433K).

Based on the above analysis, in order to predict quantitatively the dynamical properties of the PB copolymers via the CG model, a different rescaling of the CG time scale, via the ratio of the (average) friction coefficient at the atomistic scale over the CG one, for each composition should be done, since the (effective) monomeric friction coefficient of copolymers changes with the composition. Such a procedure would allow for accurate predictions of the dynamics of copolymers for each composition, but it would be of limited use since composition data for each, from atomistic simulations of PB copolymers over long times, would be required. Here, to avoid re-parametrization of the CG time at each composition, we use the standard composition mixing rules to predict the time mapping factor of the CG PB copolymer, $\tau_{CG,cop}$, as a function of the different compositions, based on the simple relation:

$$\tau_{CG,cop} = w_{cPB}\tau_{CG,cPB} + w_{tPB}\tau_{CG,tPB} + w_{vPB}\tau_{CG,vPB}$$

where w_{cPB}, w_{tPB} and w_{vPB} are the monomer compositions of cPB, tPB and vPB respectively, and $\tau_{CG,cPB}$, $\tau_{CG,tPB}$, and $\tau_{CG,vPB}$, the corresponding mapping factors of the PB homopolymers. The predictions of linear mixing rules among the three components for the time scaling factor for all copolymer systems are presented in Table SI-9 of the Supporting Information, whereas the first three lines include the corresponding values for the homopolymers.

Based on these values MSD data for segmental dynamics coming from the CG model almost collapse with the corresponding atomistic ones, apart from very short length and time scales. Results for three different PB copolymers of different compositions ({T:C:V}={34:33:33}, {25:25:50} and {10:10:80}) are presented in Figure 14a-c. Small deviations are observed, more pronounced in cm dynamics (see Figure SI-11). The size of the studied systems can be one possible reason for these discrepancies. However, given the complexity of accurately predicting the monomeric friction coefficient, these predictions are acceptable.

As an example of the aforementioned procedure, the segmental MSDs of various PB copolymers, with increasing the percentage of vinyl stereochemistry, are presented in Figure SI-12. In all cases the CG data are rescaled with the corresponding $\tau_{CG,cop}$ derived as described above (see Table SI-9)

Moreover we tested the time mapping factors through the calculation of an additional dynamical quantity, which describes orientational dynamics, in terms of the autocorellation function of the end-to-end vector. Results from both atomistic and CG simulations, scaled with the corresponding τ_{CG}, are presented in Figure SI-13a,b,c for cPB, tPB and vPB accordingly and show that scaling factors remain the same, within error bars, as the ones reported for the translational dynamics (monomeric and center-of-mass MSDs). On top of that, we examined the validity of the linear mixing rules on τ_{CG} − values, according to the Table SI-9, applied to the autocorellation function of the end-to-end vector for three copolymer systems (34:33:33; 25:25:50 and 10:10:80 in Figures SI-13d,e,f respectively). The scaling factors, which have been calculated from MSD data, are valid also for orientational dynamics, bringing the two curves close, though not in a perfect overlap.

Lastly, we should note that in the description of the atomistic model, the parameterization of the UA force field for vinyl was based on density values, whereas the dynamical properties were not taken into account. Consequently, predictions for dynamics for vinyl-1,2 PB homopolymers and vinyl-1,2 rich PB copolymers might not be in accurate agreement with experimental data. The detailed investigation of the dynamics of vPB systems is beyond the scope of the present work and will be the subject of a future work.
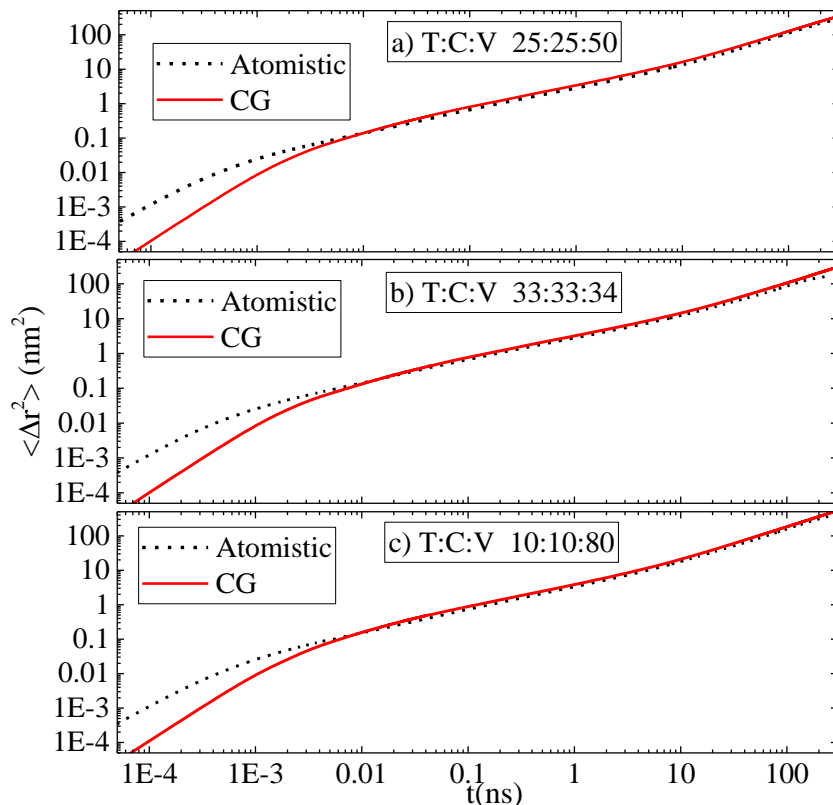
Figure 14: Mean squared displacement of monomers as a function of time for 30mer PB chains at 433K, coming from atomistic and CG model: (a) copolymer T:C:V 25:25:50; (b) copolymer T:C:V 34:33:33; (c) copolymer T:C:V 10:10:80.

5. Discussion and Conclusions

In this study we present a systematic bottom-up approach for the development of a CG model for copolymers consisting of more than one chemical species. The approach is based on a multi-component IBI optimization scheme using information from atomistic simulations of the homopolymers and one copolymer with symmetric composition. The method is applied on PB copolymers with various microstructures. CG effective potentials are developed for random PB copolymers comprised of all three isomers (cPB; tPB; vPB) via a dual-stage scheme: First, the same component terms of the CG copolymer potential are derived by simultaneously fitting bonded and non-bonded distribution functions, via IBI, for each homopolymer independently. At this point the

molecular weight transferability of the derived CG homopolymer models is thoroughly examined. Second, the CG interaction potential between different components (cross terms) are obtained by fitting the corresponding distribution functions, derived from a single PB random copolymer with an almost symmetric composition. In this stage, for the same component terms, the CG potentials from the first stage are used. The new CG model is used for CG simulations of copolymers of different composition ensuring the composition transferability. In all cases, pressure correction is also applied to accurately predict the density of the underlying model systems.

The ability of the CG model to quantitatively predict the segmental and cm dynamics of the CG PB copolymers has been thoroughly investigated. For this, a rescaling of the CG time scale, with time mapping parameter, τ_{CG}, is proposed that is related to the ratio of the atomistic over the CG monomeric friction coefficient. The τ_{CG} is calculated for the different PB homopolymers, whereas for each system, a single factor is found to describe both the segmental and cm dynamics.

Based on the above, a rough estimation of the cost efficiency of the current CG PB copolymer model, over the UA PB ones can be performed. The CG is more computationally efficient due to the following factors: 1) The smaller dimensionality of the system, since 10 atoms, or 4 united-atoms, are mapped to a single CG particle; 2) The time step for the integration of the equations of motion, which in the CG simulations is from 2fs to 5fs, compared to the 1fs used in the atomistic ones; 3) The time mapping factor which can be taken around 4.5 (as an average over all values which are predicted from the linear mixing rules). Thus, a moderate speed up factor of ~50-100 is derived, providing the opportunity for studying larger systems for longer times.

Using the derived CG model, we perform a series of CG molecular dynamics runs and explore the phase space of composition of PB copolymers in terms of cis-, trans- and vinyl proportions. Structural and dynamic measures have been calculated and discussed in comparison with the corresponding ones of PB homopolymers. Concerning the conformational/structural properties, an interesting observation is that the vinyl component strongly affects the local packing of PB copolymer melts because of its side group which impose arrangements of polymer chains at higher distances. This is obvious in the rdf of vPB homopolymer, where the first peak is moved at much larger distances

compared to both tPB and cPB ones. The packing length of vPB is also larger compared to cPB and tPB for which it attains similar values. The effect of side groups is also apparent in chain dimensions revealing the smallest R_G values for vPB compared to both other isomers; tPB is the largest one and cPB of intermediate R_G. The order is opposite for density values of homopolymers, tPB has the lowest density, vPB follows and cPB has the highest density value. Furthermore, calculation of the characteristic ratio reveals vPB as the stiffer isomer, tPB in the middle and cPB the most flexible one.

In T:C:V copolymers, using as an index the vinyl percentage, gradual decrease of chain dimensions with the increase of vinyl component is observed. However, using as an index the percentage of cis or trans, increase in chain dimensions is observed beyond 33% up to 100% homopolymer system whereas, for vinyl-rich copolymer chains R_G is considerably smaller close to the dimensions of vinyl homopolymer. Furthermore, semi-empirical rules for the prediction of the properties of random copolymers which are based on the results for homopolymers and composition (linear) mixing rules were tested. A good agreement with MD results for the radius of gyration and characteristic ratio of chains was found rendering the linear mixing model a rather good assumption for structural measures. On the other hand, the predictions of linear mixing rules underestimate the density results for copolymers.

The dynamics of un-entangled PB copolymer melts is faster than the UA PB ones, since the current CG PB copolymer models do not take into account the friction at the CG level. For this reason, a typical procedure is based on re-scaling of the CG time scale, via a time mapping factor τ_{CG}, using detailed dynamic data from the atomistic simulations. The dynamics of CG PB copolymers is found to be described via a time mapping factor, $\tau_{CG,cop}$, which can be obtain directly through standard composition mixing rules. Using $\tau_{CG,cop}$ values, which are predicted as a function of the different compositions, both segmental dynamics and cm dynamics data coming from the CG model are in rather good agreement with the corresponding atomistic ones. Based on the current model, information for dynamics mainly concerns the procedure used for the calculation of various dynamical properties of T:C:V copolymers using corresponding information from homopolymers.

A further investigation of dynamical properties, based on a model which will more accurately describe the dynamics, as well as simulations of longer polymer chains and for longer times, in order to explore the various regimes of dynamics will be the focus of a future study. Moreover we have to note here that the temperature transferability is also a very generic and important aspect in all CG models. For a rigorous systematic CG model, the CG effective interaction potentials, as parametrization of the many-body potential of mean force (free energy), are expected to depend on the actual state point (temperature and pressure).[42, 104-105] In the current work, we propose a general methodology for systematic CG models of copolymers that is transferable across molecular weight and composition range. A detailed investigation of the temperature effect on the derived CG models will be the topic of the future work.

Acknowledgements

References

1.   Akkermans, R. L. C.; Briels, W. J., Coarse-grained interactions in polymer melts: A variational approach. *The Journal of Chemical Physics* **2001,** *115* (13), 6210-6219.
2.   Akkermans, R. L. C.; Briels, W. J., A structure-based coarse-grained model for polymer melts. *The Journal of Chemical Physics* **2001,** *114* (2), 1020.
3.   Müller-Plathe, F., Coarse-Graining in Polymer Simulation: From the Atomistic to the Mesoscopic Scale and Back. *ChemPhysChem* **2002,** *3* (9), 754-769.
4.   Lahmar, F.; Rousseau, B., Influence of the adjustable parameters of the DPD on the global and local dynamics of a polymer melt. *Polymer* **2007,** *48* (12), 3584-3592.
5.   Strauch, T.; Yelash, L.; Paul, W., A coarse-graining procedure for polymer melts applied to 1,4-polybutadiene. *Physical Chemistry Chemical Physics* **2009,** *11* (12), 1942.
6.   Tschöp, W.; Kremer, K.; Batoulis, J.; Bürger, T.; Hahn, O., Simulation of polymer melts. I. Coarse-graining procedure for polycarbonates. *Acta Polymerica* **1998,** *49* (2-3), 61-74.
7.   Meyer, H.; Biermann, O.; Faller, R.; Reith, D.; Müller-Plathe, F., Coarse graining of nonbonded inter-particle potentials using automatic simplex optimization to fit structural properties. *The Journal of Chemical Physics* **2000,** *113* (15), 6264-6275.
8.   Reith, D.; Pütz, M.; Müller-Plathe, F., Deriving effective mesoscale potentials from atomistic simulations. *Journal of Computational Chemistry* **2003,** *24* (13), 1624-1636.

9.   Guerrault, X.; Rousseau, B.; Farago, J., Dissipative particle dynamics simulations of polymer melts. I. Building potential of mean force for polyethylene and cis-polybutadiene. *The Journal of Chemical Physics* **2004,** *121* (13), 6538-6546.

10.   Noid, W. G.; Liu, P.; Wang, Y.; Chu, J.-W.; Ayton, G. S.; Izvekov, S.; Andersen, H. C.; Voth, G. A., The multiscale coarse-graining method. II. Numerical implementation for coarse-grained molecular models. *The Journal of chemical physics* **2008,** *128* (24), 244115-244115.

11.   Lahmar, F.; Tzoumanekas, C.; Theodorou, D. N.; Rousseau, B., Onset of Entanglements Revisited. Dynamical Analysis. *Macromolecules* **2009,** *42* (19), 7485-7494.

12.   Lei, H.; Caswell, B.; Karniadakis, G. E., Publisher's Note: Direct construction of mesoscopic models from microscopic simulations [Phys. Rev. E81, 026704 (2010)]. *Physical Review E* **2010,** *81* (2).

13.   Maurel, G.; Schnell, B.; Goujon, F.; Couty, M.; Malfreyt, P., Multiscale Modeling Approach toward the Prediction of Viscoelastic Properties of Polymers. *Journal of Chemical Theory and Computation* **2012,** *8* (11), 4570-4579.

14.   Groot, R. D.; Rabone, K. L., Mesoscopic simulation of cell membrane damage, morphology change and rupture by nonionic surfactants. *Biophys J* **2001,** *81* (2), 725-736.

15.   Ghoufi, A.; Malfreyt, P., Coarse Grained Simulations of the Electrolytes at the Water–Air Interface from Many Body Dissipative Particle Dynamics. *Journal of Chemical Theory and Computation* **2012,** *8* (3), 787-791.

16.   Ghoufi, A.; Malfreyt, P., Mesoscale modeling of the water liquid-vapor interface: A surface tension calculation. *Physical Review E* **2011,** *83* (5), 051601.

17.   Harmandaris, V. A.; Adhikari, N. P.; van der Vegt, N. F. A.; Kremer, K., Hierarchical Modeling of Polystyrene: From Atomistic to Coarse-Grained Simulations. *Macromolecules* **2006,** *39* (19), 6708-6719.

18.   Harmandaris, V. A.; Kremer, K., Dynamics of Polystyrene Melts through Hierarchical Multiscale Simulations. *Macromolecules* **2009,** *42* (3), 791-802.

19.   Li, Y.; Abberton, B.; Kröger, M.; Liu, W., Challenges in Multiscale Modeling of Polymer Dynamics. *Polymers* **2013,** *5* (2), 751-832.

20.   Lu, L.; Dama, J. F.; Voth, G. A., Fitting coarse-grained distribution functions through an iterative force-matching method. *The Journal of Chemical Physics* **2013,** *139* (12), 121906.

21.   Mulder, T.; Harmandaris, V. A.; Lyulin, A. V.; van der Vegt, N. F. A.; Kremer, K.; Michels, M. A. J., Structural Properties of Atactic Polystyrene of Different Thermal History Obtained from a Multiscale Simulation. *Macromolecules* **2008,** *42* (1), 384-391.

22.   Spyriouni, T.; Tzoumanekas, C.; Theodorou, D.; Müller-Plathe, F.; Milano, G., Coarse-Grained and Reverse-Mapped United-Atom Simulations of Long-Chain Atactic Polystyrene Melts: Structure, Thermodynamic Properties, Chain Conformation, and Entanglements. *Macromolecules* **2007,** *40* (10), 3876-3885.

23.   Trément, S.; Schnell, B.; Petitjean, L.; Couty, M.; Rousseau, B., Erratum: "Conservative and dissipative force field for simulation of coarse-grained alkane molecules: A bottom-up approach" [J. Chem. Phys. 140, 134113 (2014)]. *The Journal of Chemical Physics* **2014,** *140* (16), 169901.

24.   Johnston, K.; Harmandaris, V., Hierarchical Multiscale Modeling of Polymer–Solid Interfaces: Atomistic to Coarse-Grained Description and Structural and Conformational Properties of Polystyrene–Gold Systems. *Macromolecules* **2013,** *46* (14), 5741-5750.

25.   Izvekov, S.; Voth, G. A., A Multiscale Coarse-Graining Method for Biomolecular Systems. *The Journal of Physical Chemistry B* **2005,** *109* (7), 2469-2473.

26.   Izvekov, S.; Voth, G. A., Multiscale coarse graining of liquid-state systems. *The Journal of Chemical Physics* **2005,** *123* (13), 134105.

27.   Hoogerbrugge, P. J.; Koelman, J. M. V. A., Simulating Microscopic Hydrodynamic Phenomena with Dissipative Particle Dynamics. *Europhysics Letters (EPL)* **1992,** *19* (3), 155-160.

28.   Klapp, S. H. L.; Diestler, D. J.; Schoen, M., Why are effective potentials soft ? *Journal of Physics: Condensed Matter* **2004,** *16* (41), 7331-7352.

29.   Kirkwood, J. G., Statistical Mechanics of Fluid Mixtures. *The Journal of Chemical Physics* **1935,** *3* (5), 300-313.

30.   Kalligiannaki, E.; Chazirakis, A.; Tsourtis, A.; Katsoulakis, M. A.; Plecháč, P.; Harmandaris, V., Parametrizing coarse grained models for molecular systems at equilibrium. *The European Physical Journal Special Topics* **2016,** *225* (8), 1347-1372.

31.   Li, Z., Stochastic many-body perturbation theory for electron correlation energies. *The Journal of Chemical Physics* **2019,** *151* (24), 244114.

32.   Rudzinski, J. F.; Noid, W. G., Coarse-graining entropy, forces, and structures. *The Journal of Chemical Physics* **2011,** *135* (21), 214101.

33.   Andersson, O., Dielectric relaxation of the amorphous ices. *Journal of Physics: Condensed Matter* **2008,** *20* (24), 244115.

34.   Deepa, M.; Bhandari, S.; Arora, M.; Kant, R., Macromol. Chem. Phys. 2/2008. *Macromolecular Chemistry and Physics* **2008,** *209* (2), 129-129.

35.   Chaimovich, A.; Shell, M. S., Anomalous waterlike behavior in spherically-symmetric water models optimized with the relative entropy. *Physical Chemistry Chemical Physics* **2009,** *11* (12), 1901.

36.   Kalligiannaki, E.; Harmandaris, V.; Katsoulakis, M. A.; Plecháč, P., The geometry of generalized force matching and related information metrics in coarse-graining of molecular systems. *The Journal of Chemical Physics* **2015,** *143* (8), 084105.

37.   Lyubartsev, A. P.; Laaksonen, A., Calculation of effective interaction potentials from radial distribution functions: A reverse Monte Carlo approach. *Physical Review E* **1995,** *52* (4), 3730-3737.

38.   Shahidi, N.; Chazirakis, A.; Harmandaris, V.; Doxastakis, M., Coarse-graining of polyisoprene melts using inverse Monte Carlo and local density potentials. *The Journal of Chemical Physics* **2020,** *152* (12), 124902.

39.   Reith, D.; Meyer, H.; Müller-Plathe, F., Mapping Atomistic to Coarse-Grained Polymer Models Using Automatic Simplex Optimization To Fit Structural Properties. *Macromolecules* **2001,** *34* (7), 2335-2345.

40.   Milano, G.; Müller-Plathe, F., Mapping Atomistic Simulations to Mesoscopic Models: A Systematic Coarse-Graining Procedure for Vinyl Polymer Chains. *The Journal of Physical Chemistry B* **2005,** *109* (39), 18609-18619.

41.   Carbone, P.; Negri, F.; Müller-Plathe, F., A Coarse-Grained Model for Polyphenylene Dendrimers: Switching and Backfolding of Planar Three-Fold Core Dendrimers. *Macromolecules* **2007,** *40* (19), 7044-7055.

42.   Qian, H.-J.; Carbone, P.; Chen, X.; Karimi-Varzaneh, H. A.; Liew, C. C.; Müller-Plathe, F., Temperature-Transferable Coarse-Grained Potentials for Ethylbenzene, Polystyrene, and Their Mixtures. *Macromolecules* **2008,** *41* (24), 9919-9929.

43.   Behbahani, A. F.; Schneider, L.; Rissanou, A.; Chazirakis, A.; Bačová, P.; Jana, P. K.; Li, W.; Doxastakis, M.; Polińska, P.; Burkhart, C.; Müller, M.; Harmandaris, V. A., Dynamics and Rheology of Polymer Melts via Hierarchical Atomistic, Coarse-Grained, and Slip-Spring Simulations. *Macromolecules* **2021,** *54* (6), 2740-2762.

44.   Pandey, Y. N.; Brayton, A.; Burkhart, C.; Papakonstantopoulos, G. J.; Doxastakis, M., Multiscale modeling of polyisoprene on graphite. *The Journal of Chemical Physics* **2014,** *140* (5), 054908.

45.   Mansky, P., Controlling Polymer-Surface Interactions with Random Copolymer Brushes. *Science* **1997,** *275* (5305), 1458-1460.

46.   Pandav, G.; Durand, W. J.; Ellison, C. J.; Willson, C. G.; Ganesan, V., Directed self assembly of block copolymers using chemical patterns with sidewall guiding lines, backfilled with random copolymer brushes. *Soft Matter* **2015,** *11* (47), 9107-9114.

47.   Rigby, D.; Lin, J. L.; Roe, R. J., Compatibilizing effect of random or block copolymer added to binary mixture of homopolymers. *Macromolecules* **1985,** *18* (11), 2269-2273.

48.   Bates, F. S.; Fredrickson, G. H., Block Copolymers—Designer Soft Materials. *Physics Today* **1999,** *52* (2), 32-38.

49.   Matsen, M. W., The standard Gaussian model for block copolymer melts. *Journal of Physics: Condensed Matter* **2001,** *14* (2), R21-R47.

50.   Vanderwoude, G.; Shi, A.-C., Effects of Blockiness and Polydispersity on the Phase Behavior of Random Block Copolymers. *Macromolecular Theory and Simulations* **2017,** *26* (1), 1600044.

51.   Fredrickson, G. H.; Milner, S. T.; Leibler, L., Multicritical phenomena and microphase ordering in random block copolymers melts. *Macromolecules* **1992,** *25* (23), 6341-6354.

52.   Angerman, H.; ten Brinke, G.; Erukhimovich, I., Fluctuation Corrections for Correlated Random Copolymers. *Macromolecules* **1998,** *31* (6), 1958-1971.

53.   Slimani, M. Z.; Moreno, A. J.; Rossi, G.; Colmenero, J., Dynamic Heterogeneity in Random and Gradient Copolymers: A Computational Investigation. *Macromolecules* **2013,** *46* (12), 5066-5079.

54.   Rissanou, A. N.; Tzeli, D. S.; Anastasiadis, S. H.; Bitsanis, I. A., Collapse transitions in thermosensitive multi-block copolymers: A Monte Carlo study. *The Journal of Chemical Physics* **2014,** *140* (20), 204904.

55.   Mao, S.; MacPherson, Q.; Qin, J.; Spakowitz, A. J., Field-theoretic simulations of random copolymers with structural rigidity. *Soft Matter* **2017,** *13* (15), 2760-2772.

56.   Deegan, R. D.; Nagel, S. R., Dielectric susceptibility measurements of the primary and secondary relaxation in polybutadiene. *Physical Review B* **1995,** *52* (8), 5653-5656.

57.   Guillermo, A.; Dupeyre, R.; Cohen-Addad, J. P., Homogeneity properties of NMR rates measured in molten polybutadiene. Temperature dependence of segmental chain motions. *Macromolecules* **1990,** *23* (5), 1291-1297.

58.   Frick, B.; Farago, B.; Richter, D., Temperature dependence of the nonergodicity parameter in polybutadiene in the neighborhood of the glass transition. *Physical Review Letters* **1990,** *64* (24), 2921-2924.

59.   Zorn, R.; Kanaya, T.; Kawaguchi, T.; Richter, D.; Kaji, K., Influence of the microstructure on the incoherent neutron scattering of glass-forming polybutadienes. *The Journal of Chemical Physics* **1996,** *105* (3), 1189-1197.

60.   Abe, Y.; Flory, P. J., Configurational Statistics of 1,4-Polybutadiene Chains. *Macromolecules* **1971,** *4* (2), 219-229.

61.   Smith, G. D.; Paul, W.; Monkenbusch, M.; Willner, L.; Richter, D.; Qiu, X. H.; Ediger, M. D., Molecular Dynamics of a 1,4-Polybutadiene Melt. Comparison of Experiment and Simulation. *Macromolecules* **1999,** *32* (26), 8857-8865.

62.   Gestoso, P.; Nicol, E.; Doxastakis, M.; Theodorou, D. N., Atomistic Monte Carlo Simulation of Polybutadiene Isomers: cis-1,4-Polybutadiene and 1,2-Polybutadiene. *Macromolecules* **2003,** *36* (18), 6925-6938.

63.   Tsolou, G.; Mavrantzas, V. G.; Theodorou, D. N., Detailed Atomistic Molecular Dynamics Simulation of cis-1,4-Poly(butadiene). *Macromolecules* **2005,** *38* (4), 1478-1492.

64.   Tsolou, G.; Harmandaris, V.; Mavrantzas, V., Temperature and Pressure Effects on Local Structure and Chain Packing in cis-1,4-Polybutadiene from Detailed Molecular Dynamics Simulations. *Macromolecular Theory and Simulations* **2006,** *15*, 381-393.

65.   Kempfer, K.; Devémy, J.; Dequidt, A.; Couty, M.; Malfreyt, P., Realistic Coarse-Grain Model of cis-1,4-Polybutadiene: From Chemistry to Rheology. *Macromolecules* **2019,** *52* (7), 2736-2747.

66.   Tow, G. M.; Maginn, E. J., Fully Atomistic Molecular Dynamics Simulations of Hydroxyl-Terminated Polybutadiene with Insights into Hydroxyl Aggregation. *Macromolecules* **2020,** *53* (7), 2594-2605.

67.   Lemarchand, C. A.; Couty, M.; Rousseau, B., Coarse-grained simulations of cis- and trans-polybutadiene: A bottom-up approach. *The Journal of Chemical Physics* **2017,** *146* (7), 074904.

68.   Hijón, C.; Español, P.; Vanden-Eijnden, E.; Delgado-Buscalioni, R., Mori–Zwanzig formalism as a practical computational tool. *Faraday Discuss.* **2010,** *144*, 301-322.

69.   Li, T.; Meng, Z.; Keten, S., Interfacial mechanics and viscoelastic properties of patchy graphene oxide reinforced nanocomposites. *Carbon* **2020,** *158*, 303-313.

70.   Guo, Y.; Liu, J.; Wu, Y.; Zhang, L.; Wang, Z.; Li, Y., Molecular insights into the effect of graphene packing on mechanical behaviors of graphene reinforced cis-1,4-polybutadiene polymer nanocomposites. *Physical Chemistry Chemical Physics* **2017,** *19* (33), 22417-22433.

71.   Zheng, Z.; Shen, J.; Liu, J.; Wu, Y.; Zhang, L.; Wang, W., Tuning the visco-elasticity of elastomeric polymer materials via flexible nanoparticles: insights from molecular dynamics simulation. *RSC Advances* **2016,** *6* (34), 28666-28678.

72.   Maurel, G.; Goujon, F.; Schnell, B.; Malfreyt, P., Multiscale Modeling of the Polymer–Silica Surface Interaction: From Atomistic to Mesoscopic Simulations. *The Journal of Physical Chemistry C* **2015,** *119* (9), 4817-4826.

73.   Pavlov, A. S.; Khalatur, P. G., Filler reinforcement in cross-linked elastomer nanocomposites: insights from fully atomistic molecular dynamics simulation. *Soft Matter* **2016,** *12* (24), 5402-5419.

74.   Pavlov, A. S.; Khalatur, P. G., Fully atomistic molecular dynamics simulation of nanosilica-filled crosslinked polybutadiene. *Chemical Physics Letters* **2016,** *653*, 90-95.

75.   Kempfer, K.; Devémy, J.; Dequidt, A.; Couty, M.; Malfreyt, P., Atomistic Descriptions of the cis-1,4-Polybutadiene/Silica Interfaces. *ACS Applied Polymer Materials* **2019,** *1* (5), 969-981.

76.   Behbahani, A. F.; Rissanou, A.; Kritikos, G.; Doxastakis, M.; Burkhart, C.; Polińska, P.; Harmandaris, V. A., Conformations and Dynamics of Polymer Chains in Cis and Trans Polybutadiene/Silica Nanocomposites through Atomistic Simulations: From the Unentangled to the Entangled Regime. *Macromolecules* **2020,** *53* (15), 6173-6189.

77.   Sadhu, S.; Bhowmick, A. K., Preparation and properties of nanocomposites based on acrylonitrile–butadiene rubber, styrene–butadiene rubber, and polybutadiene rubber. *Journal of Polymer Science Part B: Polymer Physics* **2004,** *42* (9), 1573-1585.

78.   Li, Y.; Kröger, M.; Liu, W. K., Primitive chain network study on uncrosslinked and crosslinked cis-polyisoprene polymers. *Polymer* **2011,** *52* (25), 5867-5878.

79.   Zhang, L.; Wang, Y.; Wang, Y.; Sui, Y.; Yu, D., Morphology and mechanical properties of clay/styrene-butadiene rubber nanocomposites. *Journal of Applied Polymer Science* **2000,** *78* (11), 1873-1878.

80.   Delzell, E.; Sathiakumar, N.; Hovinga, M.; Macaluso, M.; Julian, J.; Larson, R.; Cole, P.; Muir, D. C. F., A follow-up study of synthetic rubber workers. *Toxicology* **1996,** *113* (1), 182-189.

81.   Ryu, M. S.; Kim, H. G.; Kim, H. Y.; Min, K.-S.; Kim, H. J.; Lee, H. M., Prediction of the glass transition temperature and design of phase diagrams of butadiene rubber and styrene–

butadiene rubber via molecular dynamics simulations. *Physical Chemistry Chemical Physics* **2017,** *19* (25), 16498-16506.

82.   Baba, A.; Masubuchi, Y., Quantitative bridging between full-atomistic and bead-spring models for polybutadiene and poly(butadiene–styrene) copolymers. *The Journal of Chemical Physics* **2021,** *154*, 044901.

83.   Smith, G. D.; Paul, W., United Atom Force Field for Molecular Dynamics Simulations of 1,4-Polybutadiene Based on Quantum Chemistry Calculations on Model Molecules. *The Journal of Physical Chemistry A* **1998,** *102* (7), 1200-1208.

84.   Sun, H.; Ren, P.; Fried, J. R., The COMPASS force field: parameterization and validation for phosphazenes. *Computational and Theoretical Polymer Science* **1998,** *8* (1), 229-246.

85.   Polymer Data Handbook, 2nd ed. Polymer Data Handbook, 2nd ed . Edited by James E. Mark (University of Cincinnati, OH). Oxford University Press: New York. 2009 . xii + 1250 pp. $195.00. ISBN 978-0-19-518101-2. *Journal of the American Chemical Society* **2009,** *131* (44), 16330-16330.

86.   Nosé, S., A molecular dynamics method for simulations in the canonical ensemble. *Molecular Physics* **1984,** *52* (2), 255-268.

87.   Hoover, W. G., Canonical dynamics: Equilibrium phase-space distributions. *Physical Review A* **1985,** *31* (3), 1695-1697.

88.   Parrinello, M.; Rahman, A., Polymorphic transitions in single crystals: A new molecular dynamics method. *Journal of Applied Physics* **1981,** *52* (12), 7182-7190.

89.   Kotelyanskii, M., Theodorou, D. N., Simulation methods for polymers. *CRC Press* **2004**.

90.   Berendsen, H. J. C.; van der Spoel, D.; van Drunen, R., GROMACS: A message-passing parallel molecular dynamics implementation. *Computer Physics Communications* **1995,** *91* (1), 43-56.

91.   Van Der Spoel, D.; Lindahl, E.; Hess, B.; Groenhof, G.; Mark, A. E.; Berendsen, H. J. C., GROMACS: Fast, flexible, and free. *Journal of Computational Chemistry* **2005,** *26* (16), 1701-1718.

92.   Larini, L.; Lu, L.; Voth, G. A., The multiscale coarse-graining method. VI. Implementation of three-body coarse-grained potentials. *The Journal of Chemical Physics* **2010,** *132* (16), 164107.

93.   Tsourtis, A.; Harmandaris, V.; Tsagkarogiannis, D., Parameterization of Coarse-Grained Molecular Interactions through Potential of Mean Force Calculations and Cluster Expansion Techniques. *Entropy* **2017,** *19* (8), 395.

94.   Scherer, C.; Andrienko, D., Understanding three-body contributions to coarse-grained force fields. *Physical Chemistry Chemical Physics* **2018,** *20* (34), 22387-22394.

95.   Fetters, L. J.; Lohse, D. J.; Richter, D.; Witten, T. A.; Zirkel, A., Connection between Polymer Molecular Weight, Density, Chain Dimensions, and Melt Viscoelastic Properties. *Macromolecules* **1994,** *27* (17), 4639-4647.

96.   Brostow, W., Mechanical Properties. In *Physical Properties of Polymers Handbook*, Springer New York: 2007; pp 423-445.

97.   Utracki, L. A.; Simha, R.; Fetters, L. J., Solution properties of polystyrene–polybutadiene block copolymers. *Journal of Polymer Science Part A-2: Polymer Physics* **1968,** *6* (12), 2051-2066.

98.   Witten, T. A. M., S. T.; Wang, Z.-G, in Multiphase Macromolecular

Systems. *(B. M. Culbertson, editor) Plenum Press New York* **1989**.

99.   Fetters, L. J.; Lohse, D. J.; Colby, R. H. *Chain Dimensions and Entanglement Spacings: Datasheet from · Volume : "Physical Properties of Polymers Handbook" in SpringerMaterials (https://doi.org/10.1007/978-0-387-69002-5_25)*, Springer Science+Business Media, LLC.

100.   Fetters, L. J.; Lohse, D. J.; Milner, S. T.; Graessley, W. W., Packing Length Influence in Linear Polymer Melts on the Entanglement, Critical, and Reptation Molecular Weights. *Macromolecules* **1999,** *32* (20), 6847-6851.

101.   Padding, J. T.; Briels, W. J., Systematic coarse-graining of the dynamics of entangled polymer melts: the road from chemistry to rheology. *Journal of Physics: Condensed Matter* **2011,** *23* (23), 233101.

102.   Harmandaris, V. A.; Kremer, K., Predicting polymer dynamics at multiple length and time scales. *Soft Matter* **2009,** *5* (20), 3920.

103.   Ohkuma, T.; Kremer, K., Comparison of two coarse-grained models of cis -polyisoprene with and without pressure correction. *Polymer* **2017,** *130*, 88-101.

104.   Harmandaris, V. A.; Adhikari, N. P.; van der Vegt, N. F. A.; Kremer, K.; Mann, B. A.; Voelkel, R.; Weiss, H.; Liew, C., Ethylbenzene Diffusion in Polystyrene: United Atom Atomistic/Coarse Grained Simulations and Experiments. *Macromolecules* **2007,** *40* (19), 7026-7035.

105.   Rosenberger, D.; van der Vegt, N. F. A., Addressing the temperature transferability of structure based coarse graining models. *Physical Chemistry Chemical Physics* **2018,** *20* (9), 6617-6628.